Journal of Molecular Catalysis A: Chemical 352 (2012) 110–127

Contents lists available at SciVerse ScienceDirect

Journal of Molecular Catalysis A: Chemical

journal homepage: www.elsevier.com/locate/molcata

Iron(III) complexes with *meta*-substituted bis(arylimino)pyridine ligands: Catalyst precursors for the selective oligomerization of ethylene

Christian Görl*, Nadine Beck, Katharina Kleiber, Helmut G. Alt

Laboratorium für Makromolekulare Chemie, Universität Bayreuth, Universitätsstraße 30, Bayreuth D-95447, Germany

ARTICLE INFO

Article history:
Received 2 September 2011
Received in revised form 8 October 2011
Accepted 11 October 2011
Available online 18 October 2011

Keywords:
Bis(arylimino)pyridine iron complexes
Ethylene oligomerization
Oligomers
Isomerization of olefins
Branched alkenes

ABSTRACT

Bis(arylimino)pyridine iron(III) complexes containing *meta*-halogen substituents at the iminophenyl rings were synthesized and characterized. In contrast to iron(II) complexes, the presence of at least one *ortho*-substituent at the iminophenyl rings is not obligative for catalytic activities of these iron(III) complexes. After activation with methylaluminoxane (MAO), these catalysts oligomerize ethylene to give also internal and branched olefins besides the expected linear α-olefins. The widths of the resulting molecular weight distributions and the degrees of isomerization of the resulting oligomers strongly depend on the substitution pattern at the ligand frameworks.

1. Introduction

In 1998, Gibson [1–4] and Brookhart [5–7] independently reported the application of 2,6-bis(arylimino) pyridine iron complexes as effective catalysts for the polymerization and oligomerization of ethylene leading to highly linear products. The polymerization activities and the product compositions strongly depended on the substitution pattern of the iminophenyl rings [1–17]. Iron complexes bearing small substituents (alkyl or halogen) at the 2-positions of the iminophenyl rings proved to be excellent catalyst precursors for the oligomerization of ethylene to give low molecular weight α-olefins. These α-olefins are industrially highly desired compounds which are useful, e.g., for copolymerization reactions with ethylene to give linear low density polyethylene (LLDPE). In this context, halogenated 2,6-bis(arylimino)pyridine compounds play an important role as valuable ligand precursors and some of their transition metal complexes are known in the literature [1,5,8–10,14,18–29]. The introduction of such electron withdrawing substituents into the ligand backbones resulted in an enhanced temperature stability of the catalysts and consequently lead to higher activities.

While a great deal of work has been invested in bis(arylimino)pyridine iron(II) complexes, only a few publications report about the corresponding iron(III) complexes despite their higher catalytic activities towards olefin oligomerization and polymerization [14,24,29–38]. Although both iron(II) and iron(III) complexes can be undoubtedly characterized, the oxidation state of the iron centers (Fe(II) or Fe(III)) after activation with aluminoxane cocatalysts and the nature of the active species still remains unclear [4,34,39]. Actual DFT calculations by Cruz et al. [40,41] and Raucoules et al. [42] give strong evidence for the enhanced oligomerization/polymerization ability of active iron(III) species compared with iron(II) species. However, iron centers in both oxidation states may be present in the same catalyst system ("multi-centered catalysts") and lead, e.g., to polyethylenes with broad or even bimodal molecular weight distributions [40,43]. The increased activities of the bis(arylimino)pyridine iron(III) complexes can be explained with the stronger Lewis acidic character of iron(III) centers compared with iron(II) centers and, therefore, an enhanced affinity to coordinate electron rich olefin molecules. During our investigations of bis(arylimino)pyridine iron(II) and iron(III) oligomerization catalysts, we found that iron(III) catalysts usually produced mixtures of shorter chain length olefins compared to their iron(II) analogues bearing the same bis(arylimino)pyridine ligand [31,44].

One of the characteristics of the longer known 2,6-bis(arylimino)pyridine iron(II) complexes is the fact that the iminophenyl rings of the ligand frameworks must contain at least one substituent at the *ortho*-position to the iminophenyl nitrogen atoms to be stable against ligand transfer reactions. Although the synthesis of the iron(II) complex with the tridentate ligand precursor 2,6-bis(1-(phenylimino)ethyl)pyridine, a ligand without any substituents at the iminophenyl rings, was described by Abu-Surrah et al. [45], this complex probably does

* Corresponding author. Tel.: +49 921 55 2993; fax: +49 921 55 3206.
E-mail address: christian.goerl@uni-bayreuth.de (C. Görl).

1381-1169/$ – see front matter © 2011 Elsevier B.V. All rights reserved.
doi:10.1016/j.molcata.2011.10.011

not exist in the common form (L)$FeCl_2$ (L = bis(arylimino)pyridine ligand) but can be isolated as an air stable ionic compound of the composition $[(L)_2Fe]^{2+}[FeCl_4]^{2-}$. Analogous ion–pair complexes were also reported for 2,6-bis(1-(2-fluorophenyl)ethyl)pyridine [28], 2,6-bis(1-(3,5-dibromo-4-methylphenyl)ethyl)pyridine [14], 2,6-bis(1-(2,6-dibromophenyl)ethyl)pyridine [46], and 2,6-bis(1-(4-nitrophenyl)ethyl)pyridine [13]. These ion–pair complexes were catalytically completely inactive. Methyl groups seem to be the smallest *ortho*-substituents that prevent this ligand transfer reaction. In contrast to the data presented by Abu-Surrah et al. [45], Bluhm et al. [47] disclosed a different synthetic route to the neutral complex (2,6-bis(1-(phenylimino)ethyl)pyridine)$FeCl_2$ using $FeCl_2(THF)_2$ instead of the pure iron salt. The resulting complex (as well as some other described complexes) may be stabilized by the donor THF during the preparation but it showed a quite low ethylene oligomerization activity which can be explained with a fast ligand transfer reaction after activation with the cocatalyst MAO.

While the early literature mainly emphasizes the influence of substituents at the *ortho*-positions of the iminophenyl rings, more actual publications laid the focus on the *meta*- and *para*-substituents [13,14,24,29,38]. However, due to the described ligand exchange reaction, examples for 2,6-bis(arylimino)pyridine complexes bearing only substituents at the *meta*- or *para*-positions of the iminophenyl rings are still rare [38,47–52]. According to Gong et al. [36], bis(arylimino)pyridine transition metal(III) complexes without any substituents at the iminophenyl rings can be applied for the polymerization of 1,3-butadiene. The lack of substituents therefore allows the incorporation of bigger molecules than ethylene. The results of Gong et al. prompted us to investigate the stabilities of 2,6-bis(arylimino)pyridine iron(III) complexes without *ortho*-substituents at the iminophenyl rings [38]. We successfully prepared a series of such iron(III) complexes which were stable against ligand transfer reactions in contrast to the analogous iron(II) complexes [38]. Employing such iron(III) catalysts in ethylene oligomerization reactions, product mixtures with narrow molecular weight distributions were obtained [38]. However, the catalysts' thermal stabilities were lower compared with catalysts bearing *ortho*-substituents at the iminophenyl rings. Since halogen substituents at *meta*- and *para*-positions were found to increase both the catalytic activities and the thermal stabilities [13,14,24,29] we focused on the synthesis of bis(arylimino)pyridine iron(III) complexes containing *meta*-halogen substituted iminophenyl rings and the investigation of their abilities towards selective ethylene oligomerization.

2. Experimental

2.1. General considerations

All experimental work was routinely carried out using Schlenk technique. Dried and purified argon was used as inert gas. The solvents n-pentane, diethyl ether, toluene and tetrahydrofuran were purified by distillation over Na/K alloy. Diethyl ether was additionally distilled over lithium aluminum hydride, toluene was additionally dried over phosphorus pentoxide. Methylene chloride was dried over phosphorus pentoxide and calcium hydride. Methanol was dried over magnesium turnings. Drying of ethanol was accomplished with sodium. 1-Butanol (p.a.) was purchased from Merck and used without prior distillation. Methylaluminoxane (MAO) was purchased from Crompton (Bergkamen; 10% in toluene). Ethylene (3.0) and argon (4.8/5.0) were supplied by Rießner Company (Lichtenfels). All other starting materials were commercially available and were used without further purification.

NMR spectra were recorded at 25 °C on a Varian Inova 400 spectrometer. The chemical shifts in the ^1H NMR spectra are referred to the residual proton signal of the solvent (δ = 7.24 ppm for $CDCl_3$) and in ^{13}C NMR spectra to the solvent signal (δ = 77.0 ppm for $CDCl_3$). EI mass spectra were routinely recorded at the Zentrale Analytik of the University of Bayreuth with a VARIAN MAT CH-7 instrument (direct inlet, E = 70 eV) and a VARIAN MAT 8500 spectrometer. MALDI-TOF MS measurements were performed on a Bruker Daltonic Reflex TOF using graphite as matrix. The laser intensity was set to 60–70%. GC/MS spectra were recorded with a Thermo Focus gas chromatograph in combination with a Thermo DSQ mass detector (EI, 70 eV) using a HP-5MS GC column (length: 30 m, film thickness: 0.25 μm, flow: 1.5 ml/min, split ratio: 1:50) and helium as the carrier gas. The routinely used temperature program contained a starting phase (2 min at 50 °C), a heating period (10 K/min for 24 min) and a plateau phase (15 min at 290 °C) resulting in a run length of 41 min. For the analysis of oligomer mixtures, GC spectra were obtained with an Agilent 6890 N gas chromatograph equipped with a HP-5 column (length: 30 m, film thickness: 1.5 μm, flow: 150 ml/min, split ratio: 1:50). The temperature program included a starting phase (6 min at 35 °C), two heating ramps (1 K/min up to 55 °C, then 20 K/min up to 250 °C) and a plateau phase (20 min at 250 °C) resulting in a run length of 55.75 min. This temperature program allowed the separation of most of the hexene isomers. Elemental analyses were performed with a VarioEl III CHN instrument using acetanilide for calibration.

2.2. Synthesis of 3,5-dihalogen-nitrobenzenes

2,6-Dibromo-4-nitroaniline or 2,6-diiodo-4-nitroaniline (15 mmol) were dissolved in ethanol (100 ml) and cooled to 0 °C in an ice bath. Concentrated sulfuric acid (8 ml; 0.15 mol) was added dropwise over 30–45 min with constant stirring. The reaction mixture was heated to 60 °C and sodium nitrite (3.11 g; 45 mmol) was added to the reaction mixture in small portions. The resulting yellow colored reaction mixture was heated slowly to 90 °C and refluxed for 3 h whereby the color changed to brown. After cooling to room temperature, the mixture was poured into ice water. The resulting reddish brown solid was filtered off, washed with water and dried yielding the desired products as brown solid (**1**: 86%) and yellow solid (**2**: 91%), respectively.

2.3. Reduction of 3,5-dihalogen-nitrobenzenes to 3,5-dihalogenanilines

Compounds **1** or **2** (13 mmol) were dissolved in ethanol (30 ml) and $SnCl_2 \cdot 2H_2O$ (11.3 g; 50 mmol) was added portion wise at room temperature. The reaction mixtures were heated under reflux at 80 °C for 1.5 h (in case of **1**), respectively, 8 h (in case of **2**). After cooling to room temperature, the solvents were evaporated under reduced pressure and the crude solids were basified with 4N NaOH to pH 12. The mixtures were extracted with ethyl acetate (3 × 30 ml) and the combined organic layers were washed with brine and dried over sodium sulfate. The solvents were removed in vacuo providing the desired compounds as a brown solid (**3**; 86%) and a yellow solid (**4**; 89%).

2.4. Synthesis of 2,6-bis(arylimino)pyridine compounds

To a solution of 2.6-diacetylpyridine (0.49 g; 3 mmol) in toluene (20 ml) were added molecular sieves (4 Å or 3 Å; 15 g), the corresponding aniline compound (7 mmol), and the silica/alumina catalyst (0.5 g). The reaction mixture was heated to 40–45 °C for 24 h. If the reactions were not completed (according to GC/MS analyses), the heating period was prolonged till completion. After cooling to room temperature, the mixture was filtered over sodium

Table 1
^{1}H NMR, ^{13}C NMR, and MS data of compounds **1**–**16**.

Compound	^{1}H NMR δ [ppm]	^{13}C NMR δ [ppm]	MS [*m*/*z*]
1	8.29 s (2H, Ar-H), 7.96 s (1H, Ar-H)	149.0 (C_q) 140.0 (Ar-CH) 125.6 (2C, C_q), 123.4 (2C, Ar-CH)	279/281/283 $M^{\bullet+}$ (27/50/24) 235 M-NO_2 (51)200 M-Br (3) 156 M-NO_2-Br (31)
2	8.49 s (2H, Ar-H), 7.23 s (1H, Ar-H)	152.0 (C_q) 135.3 (Ar-CH), 131.8 (2C, Ar-CH), 94.2 (2C, C_q, C-I)	375 $M^{\bullet+}$ (80) 329 M-NO_2 (24) 202 M-NO_2-I (22)
3	6.98 s (1H, Ar-H), 6.71 s (2H, Ar-H), 3.74 s (br, 2H, NH_2)	148.6 (C_q), 123.6 (2C, Ar-CH), 123.3 (2C, C_q), 116.5 (Ar-CH)	249/251/253 $M^{\bullet+}$ (59/100/49) 170 M-Br (33)
4	7.16 s (1H, Ar-H), 6.91 s (2H, Ar-H), 4.71 s (br; 2H, NH_2)	149.3 (C_q), 132.4 (Ar-CH), 121.8 (2C, Ar-CH), 94.4 (2C, C_q, C-I)	345 $M^{\bullet+}$ (100) 218 M-I (47)
5	8.34 d (2H, Ar-H), 7.86 t (1H, Ar-H), 7.40–7.34 m (4H, Ar-H), 7.15–7.08 m (2H, Ar-H), 6.87–6.83 m (4H, Ar-H), 2.38 s (6H, CH_3)	167.3 (C_q, C=N), 155.4, 151.3 (C_q), 136.8 (Py-CH), 129.0, 123.6 (Ar-CH), 122.3 (Py-CH), 119.3 (Ar-CH), 16.2 (CH_3)	313 $M^{\bullet+}$ (8) 298 M-Me (2) 118 Ph-N=C-CH_3 (54) 77 Phenyl (100)
6	8.33 d (2H, Ar-H), 7.85 t (1H, Ar-H), 7.31 dd (2H, Ar-H), 6.83–6.77 m (2H, Ar-H), 6.65–6.54 m (4H, Ar-H), 2.41 s (6H, CH_3)	167.9 (C_q, C=N), 163.3 d (C_q, $^{1}J_{CF}$ = 246.1 Hz), 155.6 (C_q), 153.0 d (C_q, $^{3}J_{CF}$ = 9.2 Hz), 137.4 (Py-CH), 130.2 d (Ar-CH, $^{3}J_{CF}$ = 9.3 Hz), 123.0 (Py-CH), 115.3 d (Ar-CH, $^{4}J_{CF}$ = 2.6 Hz), 110.7 d (Ar-CH, $^{2}J_{CF}$ = 21.3 Hz), 107.0 d (Ar-CH, $^{2}J_{CF}$ = 23.1 Hz), 16.2 (CH_3)	349 $M^{\bullet+}$ (100) 239 M-[FC_6H_4N] (17) 136 FC_6H_4N=C-CH_3 (100)
7	8.31 d (2H, Ar-H), 7.85 t (1H, Ar-H), 7.28 td (2H, Ar-H), 7.08 dd (2H, Ar-H), 6.84 d (2H, Ar-H), 6.71 dd (2H, Ar-H), 2.39 s (6H, CH_3)	168.1 (C_q, C=N), 155.1, 152.4, 134.7 (C_q), 137.0 (Py-CH), 130.1, 123.7 (Ar-CH), 122.6 (Py-CH), 119.4, 117.5 (Ar-CH), 16.4 (CH_3)	381 $M^{\bullet+}$ (46) 254 M-[$ClC_6H_4NH_2$] (32) 152 ClC_6H_4N=C-CH_3 (100)
8	8.29 d (2H, Ar-H), 7.86 t (1H, Ar-H), 7.19–7.22 m (2H, Ar-H), 7.00 d (2H, Ar-H), 6.74–6.76 m (2H, Ar-H), 2.39 s (6H, CH_3)	168.1 (C_q, C=N), 155.1, 152.6, 122.7 (C_q), 136.9 (Py-CH), 130.4, 126.5 (Ar-CH) 122.6 (Py-CH), 122.2, 117.9 (Ar-CH), 16.4 (CH_3)	471 $M^{\bullet+}$ (100) 390 M-Br (11) 298 M-[$BrC_6H_4NH_2$] (55) 196 BrC_6H_4N=C-CH_3 (96)
9	8.30 d (2H, Ar-H), 7.85 t (1H, Ar-H), 7.45 dd (2H, Ar-H), 7.01–7.22 m (4H, Ar-H), 6.81 dd (2H, Ar-H), 2.39 s (6H, CH_3)	168.0 (C_q, C=N), 155.0, 152.5 (C_q), 94.4 (C_q, C-I), 136.9 (Py-CH), 132.5, 130.5, 127.9 (Ar-CH), 122.6 (Py-CH), 118.6 (Ar-CH), 16.4 (CH_3)	565 $M^{\bullet+}$ (100) 438 M-I (9) 346 M-[IC_6H_4N] (44) 244 IC_6H_4N=C-CH_3 (61)
10	8.34 d (2H), 7.86 t (1H), 7.33–7.26 m (2H, Ar-H), 7.16–7.12 m (2H, Ar-H), 6.88–6.86 m (2H, Ar-H), 6.67–6.64 m (2H, Ar-H), 2.41 s (6H, CH_3), 1.33 s (18H, t-Bu)	167.2 (C_q, C=N), 155.6, 152.2, 150.9, 34.8 (C_q), 136.8 (Py-CH), 128.6 (Ar-CH), 122.5 (Py-CH), 120.8, 116.6, 116.3 (Ar-CH), 31.3 (^{t}Bu-CH_3), 16.2 (CH_3)	425 $M^{\bullet+}$ (100) 410 M-Me (17) 368 M-tBu (14)
11	8.34 d (2H, Ar-H), 7.92 t (1H; Ar-H), 6.57–6.62 m (2H, Ar-H), 6.39–6.42 m (4H, Ar-H), 2.44 s (6H, CH_3)	168.5 (C_q, C=N), 163.5 dd (C_q, $^{1}J_{CF}$ = 246.5 Hz), 154.8 (C_q), 153.8 t (C_q, $^{3}J_{CF}$ = 9.2 Hz), 137.1, 122.9 (Py-CH), 102.4 dd (C_q, $^{2}J_{CF}$ = 22.8 Hz), 98.7 t (Ar-CH, $^{2}J_{CF}$ = 25.5 Hz), 16.4 (CH_3)	385 $M^{\bullet+}$ (13) 366 M-F (7) 154 ($F_2C_6H_3$)N≡C-CH_3 (100)
12	8.27 d (2H, Ar-H), 7.86 t (1H; Ar-H), 7.09 t (2H, Ar-H), 6.72 d (4H, Ar-H), 2.39 s (6H, CH_3)	168.7 (C_q, C=N), 154.7, 153.1 (C_q), 137.1 (Py-CH), 135.3 (C_q), 123.5, 122.9 (Ar-CH + Py-CH), 117.8 (Ar-CH), 16.5 (CH_3)	451 $M^{\bullet+}$ (7) 413 M-HCl (22) 265 M-CH_3-C≡N($C_6H_3Cl_2$) (30) 186 ($Cl_2C_6H_3$)N≡C-CH_3 (100)
13	8.23 d (2H, Ar-H), 7.82 t (1H; Ar-H), 7.35 s (2H, Ar-H), 6.88 s (4H, Ar-H), 2.35 s (6H, CH_3)	168.8 (C_q, C=N), 154.7, 153.4 (C_q), 137.1 (Py-CH), 128.9 (Ar-CH), 123.1 (C_q), 122.9 (Py-CH), 121.1 (Ar-CH), 16.6 (CH_3)	629 M^{+} (100)[a]
14	8.25 d (2H, Ar-H), 7.84 t (1H; Ar-H), 7.77 s (2H, Ar-H), 7.15 s (4H, Ar-H), 2.38 s (6H, CH_3)	168.8 (C_q, C=N), 154.7, 153.3 (C_q), 139.9 (Ar-CH), 137.1 (Py-CH), 127.4 (Ar-CH), 122.8 (Py-CH), 94.8 (C_q; C-I), 16.6 (CH_3)	817 $M^{\bullet+}$ (100)[a] 370 H_3C-C≡N-[$C_6H_3I_2$] (44)
15	8.31 d (2H, Ar-H), 7.84 t (1H; Ar-H), 6.76 dd (2H, Ar-H), 6.48 s (4H, Ar-H), 2.41 s (6H, CH_3), 2.33 s (12H; ^{t}Bu-CH_3)	167.0 (C_q, C=N), 155.5, 151.3, 138.6 (C_q), 136.7 (Py-CH), 125.2 (Ar-CH), 122.1 (Py-CH), 116.8 (Ar-CH), 21.4 (Ar-CH_3), 16.2 (CH_3)	369 $M^{\bullet+}$ (62) 354 M-CH_3 (42) 146 H_3C-C≡N-[$C_6H_3(CH_3)_2$] (100)
16	8.36 d (2H), 7.88 t (1H), 7.17 s (br, 2H, Ar-H_4), 6.71 s (br, 4H, Ar-$H_{2/6}$), 2.44 s (6H, CH_3), 1.33 s (36H, t-Bu)	167.0, 155.7, 151.5, 150.5, 34.9 (C_q), 136.8, 122.2, 117.5, 113.8 (CH), 31.5 (^{t}Bu-CH_3), 16.2 (CH_3)	537 $M^{\bullet+}$ (100) 522 M-Me (24) 480 M-tBu (57)

[a] Molecular weight too high for GC/MS analysis, thus EI-MS spectra were recorded.

sulfate, and the residue was washed several times with toluene. After removal of the solvent, methanol was added for precipitation. After storage at −20 °C for 24 h, the precipitated bis(imino)pyridine compounds were isolated and dried in vacuo. Yields: 45–85%. The analytical data for compounds **1**–**16** are given in Table 1.

2.5. General synthesis of the 2,6-bis(arylimino)pyridine iron(III) complexes *17*–*28*

An amount of 1 mmol of the 2,6-bis(arylimino)pyridine compound was dissolved in 1-butanol (20 ml; alternatively, THF or a 1:1 mixture of THF and diethylether were used) and reacted with anhydrous iron(III) chloride (1 mmol) resulting in an immediate color change to brown, orange, or red. The mixture was stirred for three hours at room temperature, whereby the complexes precipitated. n-Pentane (20 ml) was added for complete precipitation, and the mixture was stirred for another 15 min. The iron complexes were filtered over a glass frit, washed three times with 15 ml n-pentane, and dried in vacuo. Yields: 50–95%. The analytical data for complexes **17**–**28** are given in Table 2.

2.6. Oligomerization of ethylene in a 1 l Büchi autoclave

The desired iron complex (1.5–9.2 μmol) was suspended in toluene (5 ml). Methylaluminoxane (10% in toluene) was added to maintain a ratio Fe:Al = 1:2500 resulting in an immediate color change. The mixture was added to a 1 l Schlenk flask filled with 250 ml n-pentane. This mixture was transferred to a 1 l Büchi laboratory autoclave under inert atmosphere and thermostated at 60 °C.

Table 2
MS and elemental analyses data of the iron complexes **17**–**28**.

Complex	EI-MS [*m*/*z*] (rel. intensity to base peak: [%])	MALDI-TOF [*m*/*z*] (rel. intensity to base peak: [%])	Elemental analyses					
			C_{exp} [%]	C_{theor} [%]	H_{exp} [%]	H_{theor} [%]	N_{exp} [%]	N_{theor} [%]
17	474/476/478$M^{\bullet+}$ (–) 404 M-2Cl (3) 348 M-Fe-2Cl (10) 313 M-Fe-3Cl (100)	476/478 $M^{\bullet+}$ (27) 439/441 M-Cl (95) 404 M-2Cl (76) 314 [M + H]-Fe-3Cl (36)	52.88	53.03	4.25	4.03	8.76	8.84
18	510/512 $M^{\bullet+}$ (–) 475 M-Cl (6) 440 M-2Cl (14) 383 M-Fe-2Cl (8) 349 M-Fe-3Cl (100)	512/514 $M^{\bullet+}$ (20) 475/477 M-Cl (80) 440 M-2Cl (100) 405 M-3Cl (44) 350 [M + H]-Fe-3Cl (72)	49.54	49.30	3.53	3.35	8.02	8.21
19	542/544/546 $M^{\bullet+}$ (–) 509/511 M-Cl (5) 474/476 M-2Cl (3) 381 M-Fe-3Cl (47)	542/544/546 $M^{\bullet+}$ (11) 509/511 M-Cl (100) 474/476 M-2Cl (99) 381 [M + H]-Fe-3Cl (83)	46.01	46.32	3.32	3.15	7.54	7.72
20	632/634$M^{\bullet+}$ (–) 505 M-Fe-2Cl (4) 471 M-Fe-3Cl (100)	632/634/636 [M^+ (2) 595/597M-Cl (100) 561 M-2Cl (44)	40.07	39.82	2.83	2.71	6.46	6.63
21	726/728$M^{\bullet+}$ (–) 692 M-Cl (3) 600 M-I (5) 598 M-Fe-2Cl (6) 565 M-Fe-3Cl (28)	727/729/731 [$M^{\bullet+}$ + 1](16) 691/693 M-Cl (100) 656/658 M-2Cl (89) 566 [M + 1]-Fe-3Cl (29)	34.71	34.68	2.42	2.36	5.60	5.78
22	586/588 $M^{\bullet+}$ (1) 549 M-HCl (4) 537 M-Cl-Me (23) 481 M-3Cl (6) 425 M-Fe-3Cl (20)	586/588/590 $M^{\bullet+}$ (3) 571/573 M-Me (7) 570/572 M-CH_4 (24) 551/553 M-Cl (48) 516 M-2Cl (100)	59.53	59.26	5.89	6.00	7.14	7.15
23	546/548 $M^{\bullet+}$ (–) 385 ligand (78) 154 $F_2(C_6H_3)N{\equiv}C\text{-}CH_3$ (100)	547/549 [M + 1] (1) 511 M-Cl (100) 476 M-2Cl (62) 384 M-Fe-3Cl (2)	45.73	46.06	2.87	2.76	7.49	7.67
24	610/612 $M^{\bullet+}$ (–) 541 M-2Cl (1) 451 ligand (50) 416 ligand-Cl (33)	613/611 [M + 1] (8/13) 576 M-Cl (100) 541 M-2Cl (61) 506 M-3Cl (30) 452 [M + 1]-Fe-3Cl (33) 451 M-Fe-3Cl (14)	40.88	41.12	2.71	2.46	6.63	6.85
25	790/792 $M^{\bullet+}$ (–) 629 ligand (10) 547 ligand-Br (6)	794/792 $M^{\bullet+}$ (6) 757/755 M-Cl (95/100) 722 M-2Cl (22) 628 M-Fe-3Cl-H (6)	31.57	31.88	2.02	1.91	5.18	5.31
26	978/980 $M^{\bullet+}$ (–) 817 ligand (2) 343 [$I_2C_6H_3N$] (82)	978/980 $M^{\bullet+}$ (2) 945/943 M-Cl (78/100) 908/910 M-2Cl (9/35) 816 M-Fe-3Cl (3)	25.72	25.76	1.72	1.54	4.28	4.29
27	530/532 $M^{\bullet+}$ (–) 495 M-Cl (3) 369 ligand (100)	530/532 $M^{\bullet+}$ (2) 495 M-Cl (33) 461 M-Cl-HCl (100) 426 M-3Cl (34) 368 M-Fe-3Cl-H (31)	51.95	52.19	5.18	5.12	6.79	6.90
28	698/700 $M^{\bullet+}$ (1) 665 M-Cl (19) 662 M-HCl (38) 628 M-2Cl (3) 595 M-3Cl (2) 537 M-Fe-3Cl (100) 480 M-t-Bu-$FeCl_3$ (77)	698/700/702 $M^{\bullet+}$ (30) 665 M-Cl (80) 629 M-Cl-HCl (100) 595 M-3Cl (14)	63.78	63.48	7.37	7.34	5.89	6.00

An ethylene pressure of 10 bar was applied and the mixture was stirred for one hour, then the ethylene flow was stopped. After cooling down to −15 °C, the ethylene pressure was carefully released (with loss of traces of butenes and no loss of oligomers ≥ C_6). A sample (1 ml) was taken from the cooled mixture by syringe and filtered over a small silica column which was externally cooled with an isopropanol/dry-ice bath (−20 °C). From the filtered solution, a volume of 2 μl was applied for the GC analysis. The relative ratios of the oligomer fractions (C_4, C_6, C_8) could be taken from the gas chromatogram. The GC temperature program was optimized especially to display the separation of the C_6 isomers. For a quantitative analysis of the C_6 fraction, diluted hydrochloric acid (20 ml of a 1 M HCl) was slowly added to the whole oligomer mixture. The resulting biphasic system was then allowed to come to room

temperature whereby most of the butenes were evolved. The oligomer solution was separated and dried over sodium sulfate. The residual butenes and the solvent n-pentane were carefully distilled off using a Vigreux column ($T_{external\ bath}$ = 40 °C). The residue (containing the C_6 and higher oligomers and a small amount of toluene from the MAO) was heated slowly, and the C_6 fraction was collected (at $T_{external\ bath}$ = 65–70 °C) and weighed after cooling down to room temperature. From the corresponding GC integral of the C_6 fraction (thus serving as an internal standard), the amounts of the C_4 and C_8 fractions were then calculated. Due to the similar boiling points of toluene (111 °C) and the octene isomers (~110–125 °C), a separation of the C_8 fraction by distillation could not be accomplished.

3. Results and discussion

3.1. Synthesis of meta-dihalogen substituted anilines

While many *meta*-halogen substituted aniline derivatives are readily commercially available, 3,5-dibromoaniline and 3,5-diiodoaniline had to be prepared in a two-step synthesis. Diazotation of the amino groups of 2,6-dibromo-4-nitroaniline and 2,6-diiodo-4-nitroaniline was accomplished using an excess of sodium nitrite and sulfuric acid (96 wt.%). Subsequent removal of the diazo function by heating the reaction mixture for three hours at 90 °C lead to the 3,5-dihalogen-nitrobenzenes **1** and **2** (Scheme 1) [53].

Reduction of compounds **1** and **2** was achieved applying $SnCl_2{\cdot}2H_2O$ as the reducing agent obtaining the desired 3,5-dihalogenanilines **3** and **4** in high yields (Scheme 1) [53].

3.2. Preparation of substituted 2,6-bis(arylimino)pyridine compounds

Condensation reactions of 2,6-diacetylpyridine with *meta*-halogen substituted anilines yielded the 2,6-bis(arylimino)pyridine compounds (Scheme 2). For comparison purposes, some ligand precursors were prepared using *meta*-alkyl substituted anilines. Condensation reactions using 3-methylaniline (m-toluidine) as the amine compound surprisingly did not lead to the desired bis(arylimino)pyridine compound but gave condensation products of the aniline. 2,6-Bis(arylimino)pyridine compounds containing electron withdrawing substituents on their iminophenyl rings were found to be much more sensitive towards air and moisture (easy hydrolysis of the imine groups!) compared with alkyl or aryl substituted analogues. Additionally, the iodo substituted ligand precursors appeared to be light sensitive. Former literature usually reported the use of *para*-toluenesulfonic acid as a catalyst for the condensation reactions of 2,6-diacetylpyridine with aniline derivatives [2,5,54]. The great disadvantage of this method is the comparably high reaction temperature of about 130 °C due to azeotropic water removal using a Dean–Stark trap and the poor solubility of *para*-toluenesulfonic acid in toluene at lower temperatures. As a result, some temperature sensitive anilines decomposed under these quite harsh reaction conditions and did not provide the desired bis(arylimino)pyridine compounds. To overcome these problems, an elegant method introduced by Qian et al. [8,55] was applied using a heterogeneous silica/alumina catalyst (13% Al_2O_3/87% SiO_2) and molecular sieves 3 Å as the water absorbing agent. The heterogeneous catalyst acts as a Lewis acid and, additionally, as a scavenger for impurities in the aniline compounds. Due to the lower reaction temperatures (40–45 °C), no decomposition products were found in the reaction mixtures and the bis(imine) compounds could be readily isolated. Table 3 gives an overview of the prepared 2,6-bis(arylimino)pyridine compounds, while the ^{1}H NMR, ^{13}C NMR, and MS data for compounds **5**–**16** can be found in Table 1 (see Section 2).

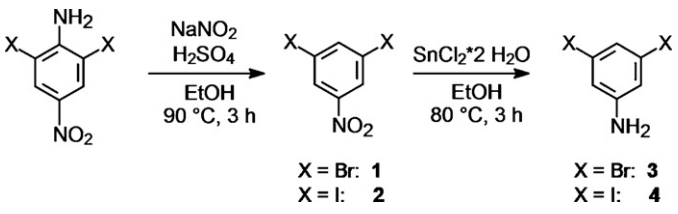

Scheme 1. Synthesis of 3,5-dibromo- and 3,5-diiodoaniline.

3.3. Synthesis of the iron(III) complexes

The bis(arylimino)pyridine compounds **5**–**16** were reacted with anhydrous ferric chloride either in n-butanol or a 1:1 (v:v) mixture of diethylether and THF to give the corresponding bis(arylimino)pyridine iron(III) complexes **17**–**28** (Scheme 3 and Table 3) which could be isolated as orange or brown solids.

As described in the introduction chapter, many bis(arylimino)pyridine compounds without or with small substituents at the *ortho*-positions of the iminophenyl rings immediately form deep purple or violet ion–pair complexes $[L_2Fe]^{2+}$ $[FeCl_4]^{2-}$ in reactions with iron(II) chloride. However, in some cases, the iron(II) complexes seem to exist as (L)$FeCl_2$ type complexes when bearing 4-iodo [29], 4-allyl [56], 3-vinyl [52], 3- or 4-trifluoromethyl [47], or 3- or 4-methoxy [47] substituted iminophenyl rings.

In contrast, reactions of such bis(arylimino)pyridine compounds with iron(III) chloride cleanly provided the desired mono-ligated complexes of the general formula (L)$FeCl_3$ [38]. However, the resulting complexes are not stable towards ligand transfer reactions when they are kept in polar solvents (like THF or alcohols, see Refs. [14] and [34]) for some hours. Additionally, at longer reaction times these iron(III) complexes can act as oxidation reagents towards the solvent THF resulting in the abstraction of hydrogen atoms, the loss of HCl, and the formation of the corresponding iron(II) complexes [57–59]. Therefore, the time limit for the complexation reactions and the subsequent isolation procedures was determined to about three hours. All complexes were stored in the dark to prevent the iron(III) centers from reduction to iron(II), as light also seemed to have a detrimental influence on the complex stabilities.

The iron(III) complexes were characterized by mass spectrometry (EI-MS and MALDI-TOF MS) and elemental analyses. Compared with the analogous iron(II) complexes, the iron(III) complexes are less stable to fragmentation in EI-MS, so in most cases the molecular ion was not detectable. In contrast, MALDI-TOF MS analyses gave more significant results and the molecular ions were found for all complexes. As expected, mass distributions due to the presence of chloro atoms (and in some cases additionally bromo atoms) were obtained. Due to their paramagnetism, ^{1}H NMR analyses of these iron complexes appeared to be less significant, since no defined signals could be found in the range between −2000 and 2000 ppm (relative to Me_4Si). The MS and elemental analyses data are given in Table 2.

Scheme 4 shows the MALDI-TOF mass spectrum of complex **21**. Around m/z = 728, the molecular ion mass distribution was observed. The base peak at m/z = 691/693 resulted from the loss of one chloro ligand, while the ion at m/z = 656/658 had its origin in the loss of two chloro ligands. At m/z = 566, an ion corresponding to the protonated ligand [M_{ligand} + 1] was detected.

While for complex **21** the molecular ion in the MALDI-TOF mass spectrum was clearly visible, the intensities of the molecular ions of 2,6-bis(arylimino)pyridine iron complexes bearing dihalogenated iminophenyl rings were distinctively lower but the ways of decomposition are identical. Scheme 5 shows the upper mass region of

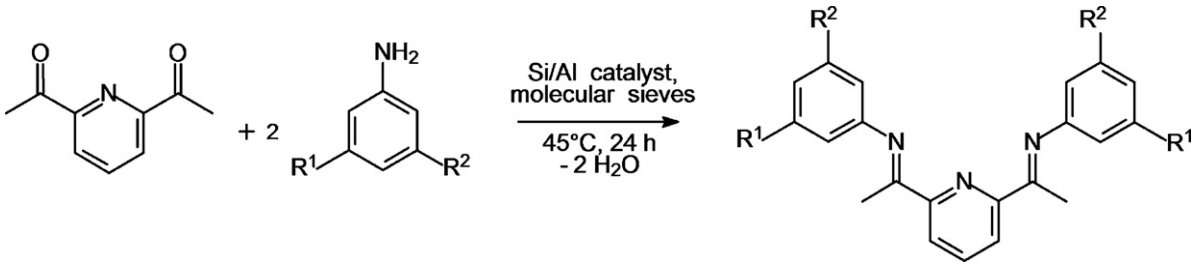

Scheme 2. General synthesis of 2,6-bis(arylimino)pyridine compounds **5**–**16**.

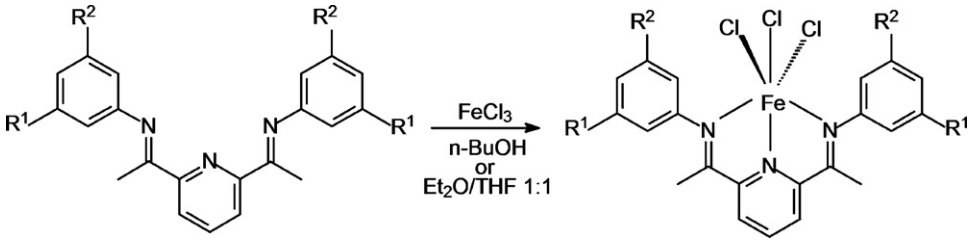

Scheme 3. Synthesis of the bis(arylimino)pyridine iron complexes **17**–**28**.

Table 3
Synthesized 2,6-bis(arylimino)pyridine compounds and their corresponding iron(III) chloride complexes (yields given in brackets).

Bis(imino) compound	R^1	R^2	Iron(III) complex
5 (77%)	H	H	**17** (94%)
6 (56%)	**F**	H	**18** (95%)
7 (74%)	**Cl**	H	**19** (83%)
8 (73%)	**Br**	H	**20** (74%)
9 (54%)	**I**	H	**21** (65%)
10 (69%)	**t-Bu**	H	**22** (49%)
11 (55%)	**F**	**F**	**23** (69%)
12 (54%)	**Cl**	**Cl**	**24** (59%)
13 (55%)	**Br**	**Br**	**25** (79%)
14 (47%)	**I**	**I**	**26** (65%)
15 (68%)	**Me**	**Me**	**27** (82%)
16 (85%)	**t-Bu**	**t-Bu**	**28** (68%)

the MALDI-TOF mass spectrum of complex **26** (diiodo substituted iminophenyl rings) including a closer look at the region $m/z = 900$ up to $m/z = 1000$ while Scheme 6 shows the isotope distributions of the molecular ion around $m/z = 979$ and of the base peak (loss of HCl or Cl) around $m/z = 943$.

Similarly to complexes **21** and **26**, MALDI-TOF mass spectra for all other complexes revealed that the base peaks result from the loss of either one or two chloro ligands (see Table 2).

Slow diffusion of toluene into a dichloromethane solution of complex **21** afforded thin orange brown colored needles. However, due to their geometry these crystals were found to be unsuitable for X-ray analyses. Similarly to the three literature known crystal structures of bis(arylimino)pyridine iron(III) complexes [14,30,36], the *R* value was too high (corresponding to an increased uncertainty for the geometry of the molecule). Finally, the refinement procedure could not be finished successfully.

3.4. Results of the catalytic oligomerization of ethylene

3.4.1. Oligomerization activities and product molecular weight distributions

The iron complexes **17**–**28** were applied as catalyst precursors for the homogeneous oligomerization of ethylene. The complexes were activated with methylaluminoxane (MAO) applying a ratio Fe:Al = 1:2500. Oligomerization runs were routinely performed in a 1 l Büchi steel reactor at a temperature of 60 °C over one hour employing an ethylene pressure of 10 bar. As a solvent n-pentane was used. Due to the big differences in their activities, the complexes were used in appropriate molar amounts to keep the exothermic reaction under control. Depending on the size and the nature of the substituents at the iminophenyl rings, a wide range of olefinic products were obtained from the activated complexes **17**–**28**. Their oligomerization results are given in Table 4 while Table 5 provides a detailed comparison of the most relevant oligomerization properties of *ortho*-, *meta*-, di-*meta*-, and *para*-halogen substituted bis(arylimino)pyridine iron(III) catalysts including some results of our previous study [38].

In all experiments, the product mixtures mainly consisted of low molecular weight α-olefins and, to a lower extent, of internal and branched olefins. No solid products (=polyethylenes) were obtained. The oligomer mixtures were characterized by gas chromatography and GC/MS correlations using the NIST mass spectral database. The C_6 fractions were isolated and weighed (thus serving as an internal standard), and the amounts of butenes and octenes were then calculated from the corresponding

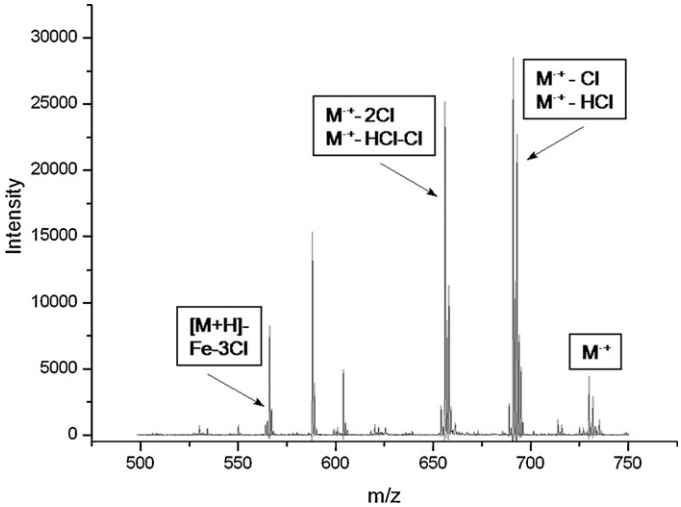

Scheme 4. MALDI-TOF mass spectrum of complex **21** with clearly visible molecular ion around $m/z = 729$ (ions with $m/z < 500$ were omitted for clarity).

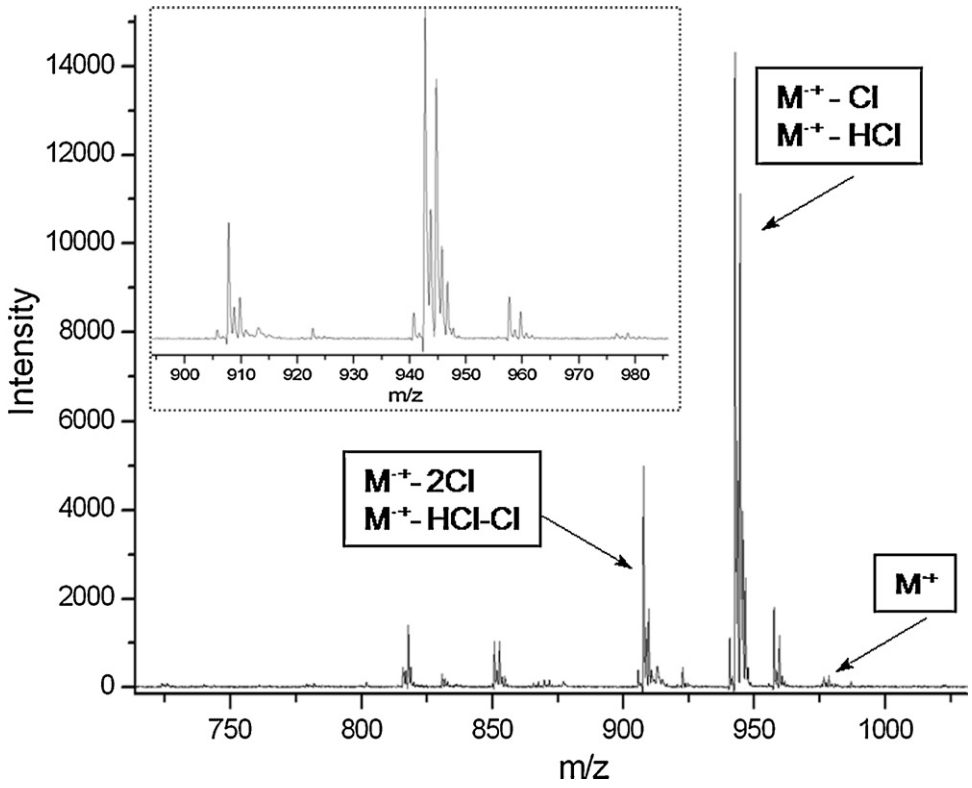

Scheme 5. MALDI-TOF mass spectrum of complex **26** with less intensive molecular ion around $m/z = 979$ (ions with $m/z < 700$ were omitted for clarity). Offset: enlarged view of the region $m/z = 900$ up to $m/z = 1000$.

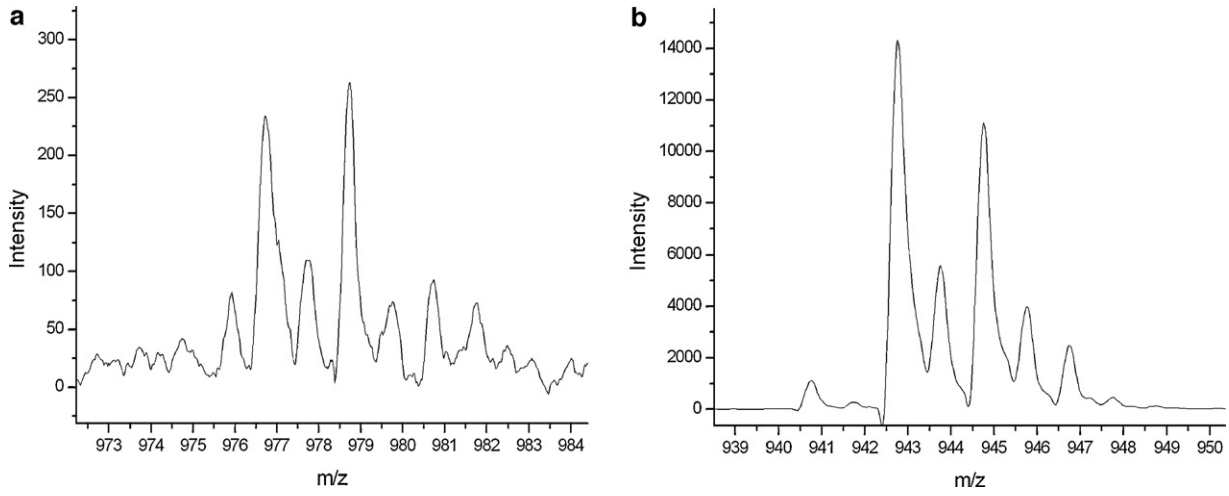

Scheme 6. Enlarged sections of the MALDI-TOF mass spectrum of complex **26**: (left) isotope distribution of the molecular ion M^+ around $m/z = 979$ and (right) ion distribution around $m/z = 943$ for the loss of HCl or Cl.

GC integrals. The catalysts' activities were calculated both from the consumed amount of ethylene (named as "theoretical yield" in Table 4) and from the obtained amount of C_6 oligomers (given as "oligomer yield" in Table 4). Remarkably, the activities determined from weighing the C_6 fractions are only marginally lower (1–5%) compared with the values calculated from the ethylene consumptions which indicates that the workup procedure (see Section 2) sufficiently retains the butenes in the mixtures).

The Schulz–Flory coefficient α was found to be a useful parameter for the description of the product compositions, i.e., the molecular weight distributions of the oligomer mixtures [60–66]. It can be calculated from both the reaction rate constants and the GC integrals of the oligomer fractions. Since the GC integrals are easily accessible and are related to the molar amounts of the oligomers, α can be defined as the quotient of the molar amounts of two subsequent oligomer fractions whose carbon numbers differ by a number of 2:

$$\alpha = \frac{k_{\text{propagation}}}{k_{\text{propagation}} + k_{\text{termination}}} = \frac{\text{mol}(C_{n+2})}{\text{mol}(C_n)} \quad (1)$$

$k_{\text{propagation}}$ and $k_{\text{termination}}$ describe the rate constants for chain growth and chain termination. C_n and C_{n+2} rely to olefins with n or $(n+2)$ carbon atoms giving α as the average value of at least two subsequent propagation steps. In the present study, the $C_6 \rightarrow C_8$

Table 4
Ethylene oligomerization results for the iron complexes **17–28** (solvent: 250 ml n-pentane, activator: MAO, Fe:Al = 1:2500, T = 60 °C, 10 bar ethylene, 1 h).

Complex	n_{Cat} [μmol]	Ethylene consumption [l]	Theoretical yield [g]	Oligomer yield [g][a]	Activity [kg prod./mol Fe h]	C[b]	M[c] [g/mol]	Oligomer yield [mol]	Schulz–Flory coefficient α	C_4 olefins in the product mixture			1-butene in the	
										[%]	[g][a]	[mol][a]	product mixture [%]	C_4 fraction [%]
17	9.2	32.2	38.7	38.5	4150	6.03	84.5	0.46	0.28	29.3	7.5	0.13	29.0	98.9
18	6.1	44.4	53.3	52.9	7320	6.14	87.7	0.61	0.36	35.7	12.1	0.22	35.1	98.3
19	2.0	87.7	105.3	104.2	52050	5.59	78.4	1.33	0.29	41.0	30.6	0.55	40.5	98.8
20	1.6	29.0	34.8	34.4	22000	4.99	70.0	0.49	0.27	60.9	16.9	0.30	60.6	99.6
21	4.1	65.4	78.5	78.0	19070	6.15	86.3	0.76	0.36	34.5	14.7	0.26	34.1	98.9
22	4.7	31.1	38.7	37.1	7900	5.57	78.2	0.48	0.23	41.5	11.0	0.20	41.2	99.3
23	3.7	18.8	22.9	22.5	6025	5.09	71.4	0.32	0.28	57.9	10.2	0.18	57.5	99.3
24	2.3	39.4	47.3	46.5	20650	5.69	79.8	0.59	0.35	42.9	14.3	0.25	42.6	99.5
25	1.5	56.0	67.6	67.0	44480	5.25	73.7	0.91	0.33	53.1	27.1	0.48	52.7	99.3
26	2.3	20.4	24.6	24.4	10420	5.96	83.6	0.29	0.35	48.4	7.9	0.14	48.2	99.7
27	2.4	8.8	10.5	10.2	4270	5.33	74.8	0.14	0.23	46.6	3.5	0.06	46.4	99.6
28	3.1	53.6	64.3	64.0	20400	5.50	77.2	0.83	0.20	41.1	19.1	0.34	41.1	>99.9

Complex	C_6 olefins in the product mixture			1-hexene in the		C_8 olefins in the product mixture			1-octene in the		C_{10} olefins in the product mixture [%]	Higher oligomers [%]
	[%]	[g][d]	[mol][d]	product mixture [%]	C_6 fraction [%]	[%]	[g][a]	[mol][a]	product mixture [%]	C_8 fraction [%]		
17	49.5	19.0	0.23	24.4	49.3	14.7	7.5	0.07	9.4	55.2	4.4	2.3
18	38.9	19.8	0.24	21.9	51.9	13.4	9.1	0.08	9.5	71	5.7	6.3
19	39.0	43.6	0.52	26.4	68.6	10	14.9	0.13	8.2	82	3.2	6.8
20	29.8	12.4	0.15	24.3	80.8	5.8	3.2	0.03	5.5	96.2	2	1.5
21	41.1	26.2	0.31	22.8	55.4	13.1	11.1	0.1	10	76.6	5.5	5.8
22	45.1	18.0	0.22	29.4	64.8	10.5	5.6	0.05	9.9	82.9	2.3	0.6
23	30.8	8.2	0.10	25.5	82.8	7.6	2.7	0.02	7.1	93.9	2.4	1.3
24	35.6	17.8	0.21	27.3	76.7	12.8	8.5	0.07	11.7	91.8	4.4	7.3
25	29.4	22.5	0.27	22.4	76.4	8.7	8.9	0.08	7.9	90.9	3.3	5.5
26	33.2	8.1	0.09	27.4	82.6	10.7	3.5	0.03	10.4	97.9	4	3.7
27	41.2	4.6	0.05	32.1	77.8	8.7	1.3	0.01	8.7	100	2.3	1.2
28	45.9	32.0	0.38	32.1	70	11.4	10.6	0.09	10.4	91.2	2.6	–

[a] Yields for the C_4 and C_8 fractions calculated using the C_6 fraction as "internal standard".
[b] Average carbon number of the oligomer mixture (in analogy to the average polymerization grade defined by Henrici-Olive and Olive in Ref. [66]) calculated from the GC integrals.
[c] Average molecular weight of the oligomer mixture (M = C × 14.027 since the olefins can be expressed as C_nH_{2n}).
[d] Yields for the C_6 fractions were weighed.

Table 5
Comparison of Schulz–Flory values, the overall contents of C_6 olefins, and the amount of 1-hexene within the C_6 fractions of *ortho*-, *meta*, di-*meta*-, and *para*-halogen or -alkyl substituted 2,6-bis(arylimino)pyridine iron(III) complexes (compounds noted in brackets could not be obtained, therefore no values can be given).

	Substituent at the iminophenyl ring in position							
	ortho		meta		di-meta		para	
Schulz–Flory coefficient α	2-F	0.71	18 (3-F)	0.36	23 (3,5-di-F)	0.28	4-F	0.43
	2-Cl	0.91	19 (3-Cl)	0.29	24 (3,5-di-Cl)	0.35	4-Cl	0.29
	2-Br	0.97	20 (3-Br)	0.27	25 (3,5-di-Br)	0.33	4-Br	0.28
	[2-I]	–	21 (3-I)	0.36	26 (3,5-di-I)	0.35	4-I	0.38
	17 (2-H)	0.27	22 (3-^{t}Bu)	0.23	28 (3,5-di-^{t}Bu)	0.20		
	2-Me	0.78	[3-Me]	–	27 (3,5-di-Me)	0.23		
C_6 olefins in the product mixture [%]	2-F	32.4	18 (3-F)	38.9	23 (3,5-di-F)	30.8	4-F	41.7
	2-Cl	16.2	19 (3-Cl)	39.0	24 (3,5-di-Cl)	35.6	4-Cl	54.0
	2-Br	9.3	20 (3-Br)	29.8	25 (3,5-di-Br)	29.4	4-Br	51.5
	[2-I]	–	21 (3-I)	41.1	26 (3,5-di-I)	33.2	4-I	46.0
	17 (2-H)	49.5	22 (3-^{t}Bu)	45.1	28 (3,5-di-^{t}Bu)	41.2		
	2-Me	4.4	[3-Me]	–	27 (3,5-di-Me)	45.9		
1-hexene in the C_6 fraction [%]	2-F	46.8	18 (3-F)	51.9	23 (3,5-di-F)	82.8	4-F	41.5
	2-Cl	>99	19 (3-Cl)	68.6	24 (3,5-di-Cl)	76.7	4-Cl	49.3
	2-Br	>99	20 (3-Br)	80.8	25 (3,5-di-Br)	76.4	4-Br	49.3
	[2-I]	–	21 (3-I)	55.4	26 (3,5-di-I)	82.6	4-I	45.9
	17 (2-H)	49.3	22 (3-^{t}Bu)	64.8	28 (3,5-di-^{t}Bu)	77.8		
	2-Me	93.7	[3-Me]	–	27 (3,5-di-Me)	70.0		

and the $C_8 \rightarrow C_{10}$ propagation steps were used for the calculation of α.

A higher value of the Schulz–Flory coefficient α directly corresponds to an increased propagation probability resulting in higher molecular weight products. The upper limit $\alpha = 1$ is only reached when molecular weight distributions are obtained in which the maximum peak appears at higher carbon numbers (usually butenes or hexenes are the main products) but in these cases the mathematical requirements for a Schulz–Flory distribution are not fulfilled (an ideal Schulz–Flory distribution is obtained for $\alpha \sim 0.7$). Eq. (1) shows that higher values for α are equivalent to increased amounts of higher olefins in the product mixtures. Since such mixtures can be hardly separated, it is desirable to design more selective catalysts. Many efforts have been made especially to prepare catalysts which selectively produce, e.g., only 1-hexene or 1-octene, since these α-olefins are consumed in large amounts as comonomers in the synthesis of linear low density polyethylenes (LLDPE). At present, chromium catalysts based on [PNPN] ligands represent the upper limit for the selective trimerization of ethylene to give 1-hexene [67] and references therein]. For the catalysts **17**–**28**, narrow molecular weight distributions were observed with $\alpha < 0.40$ (see Table 4).

For almost all oligomerization runs, very high initial ethylene uptake rates could be observed (up to 10 l of ethylene/min). Due to the gradual catalyst degradation, the ethylene flows drop distinctively during the experiments, and for the systems **17**/MAO and **18**/MAO the ethylene flow had ceased before the end of the regular run time (1 h). Complex **17** which was described to be catalytically active in the polymerization of 1,3-butadiene [36], exhibited a moderate activity in ethylene oligomerization (4150 [kg prod./mol Fe h]). However, due to its lack of any substituents at the iminophenyl rings, complete deactivation had to be noted after a run time of only 10 min when no more ethylene was consumed. The Schulz–Flory coefficient α was determined to $\alpha = 0.28$ indicating a very narrow product distribution. Regarding the fast deactivation of **17**, complexes bearing *meta*- or *para*-halogen substituted iminophenyl rings were considered to exhibit an improved shield of the iron center [38]. The oligomerization results of the iron(III) complexes **18**–**21** with *meta*-substituted bis(arylimino)pyridine ligands revealed that mainly butenes, hexenes, and octenes were produced, and the contents of higher alkenes did not exceed 12 wt.% (Table 4).

The oligomerization activities of complexes **18**–**21** exhibited distinct differences. Analogously to the *ortho*-substituted catalysts [38], the 3-chloro derivative **19** showed an extremely high activity of 52050 [kg prod./mol Fe h] which is distinctively higher compared with the 3-fluoro, 3-bromo, and 3-iodo derivatives **18**, **20**, and **21**. Actually, **19** is the most active bis(arylimino)pyridine iron catalyst which does not contain any substituents at the *ortho*-positions to the former amino nitrogen atoms. While the high electronegativity of the chloro substituents leads to a decrease of the electron density in the iminophenyl rings, the "medium"-sized chloro atoms apparently leave enough space for the coordination of ethylene molecules to the iron centers and for the growing chain, whereas the *meta*-bromo atoms may partially interfere with incoming ethylene molecules leading to a lower activity (22000 [kg prod./mol Fe h]). The comparatively low activity of the 3-fluoro substituted complex **18** could be explained with a faster deactivation of the catalytically active centers due to the above described ligand transfer reaction. A visible proof of that assumption was the purple color of the resulting oligomer mixture due to the octahedrally coordinated Fe^{3+} ions which are bonded to the six nitrogen atoms of the two bis(arylimino)pyridine ligands (see Scheme 7).

The small size of the fluoro atoms and the polar structure of the activated catalyst molecules favors this ligand transfer reaction, so its rate constant becomes dominant over the rate constant of ethylene insertion. The neutral bis(arylimino)pyridine iron(III) complexes are stable against this ligand transfer reaction; it only occurs after activation of the complexes with MAO in competition to the chain propagation reaction (see Scheme 7). Due to the abstraction of an iron-methyl group, the activated cationic iron(III) complexes are structurally similar to neutral bis(arylimino)pyridine iron(II) complexes which could only be isolated as ion pairs when the ligand framework consisted of exclusively *meta*- or *para*-substituted iminophenyl rings (with the above mentioned rare exceptions [29,47,51,52]).

Among the *para*-halogen substituted complexes, the iodo derivative exhibited the highest activity (22825 [kg prod./mol Fe h], see [38]) while for the fluoro, chloro, and bromo derivatives activities lower than 5000 [kg prod./mol Fe h] were observed. Therefore, an improved shield of the iron center can be considered for the *meta*-halogen substituted catalysts compared with the *para*-substituted analogues. The beneficial effect of introducing iodo substituents at the *para*-positions of bis(arylimino)pyridine ligands

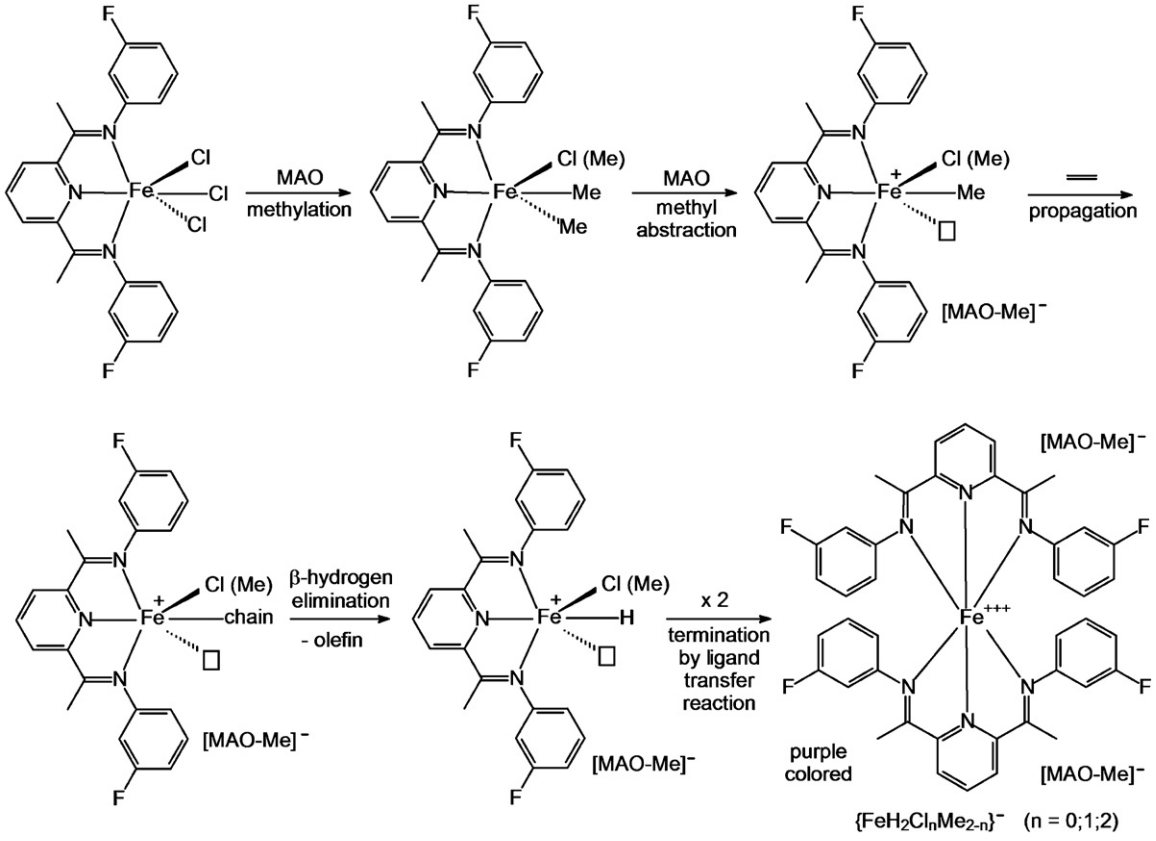

Scheme 7. Activation of complex **18** with MAO and termination by ligand transfer reaction. [MAO-Me]⁻ describes the MAO cages which act as counter anions.

[29] can be explained with the size and the good polarizability of the voluminous iodo atoms due to partial compensation of the positive charges at the iron centers during the oligomerization process ("electronical flexibility", see [30] and [68]).

The product mixtures obtained with catalysts **18**–**21/MAO** bearing *meta*-halogen substituted ligands exhibited α values in the range 0.27–0.36 indicating narrow molecular weight distributions. These values are similar to those obtained for the corresponding *para*-substituted catalysts and much lower than those of the *ortho*-substituted iron(III) catalysts (see Table 5 and [38]) for which the Schulz–Flory coefficients α increased with increasing the size of the *ortho*-halogen substituent (**2-F**: $\alpha = 0.71$ < **2-Cl**: $\alpha = 0.91$ < **2-Br**: $\alpha = 0.97$; the complexation reaction to give the 2-iodo substituted iron(III) complex failed). While the overall contents of C_4, C_6, and C_8 olefins for the fluoro, chloro, and iodo derivatives **18**, **19**, and **21** were very similar (~35%, 39%, 10%), the bromo substituted compound **20** mainly produced 1-butene and less hexenes and octenes. For the *meta*-dihalogen substituted catalysts **23**–**26**, the overall contents of C_6 olefins were somewhat lower compared with catalysts **18**–**21** corresponding to an enhanced steric bulk around the iron centers. According to Table 5, the contents of C_6 olefins roughly increase in the order *ortho*- < di-*meta*- < *meta*- < *para*-halogen substitution.

Among the *meta*-dihalogen substituted bis(arylimino)pyridine iron catalysts **23–26** the bromo compound **25** revealed to be the most active candidate (44480 [kg prod./mol Fe h]). The Schulz–Flory coefficients α for the dihalogen substituted catalysts **23**–**26** were found in the same range as for the mono-halogen compounds **18**–**21**. Similarly to the mono-bromo derivative **20**, **25**/MAO produced a distinctively higher amount of butenes (Schulz–Flory coefficient $\alpha = 0.33$) and less amounts of the higher olefins compared with the difluoro, dichloro, and diiodo substituted catalysts **23**, **24**, and **26**. In analogy to **18**, the low activity of the 3,5-difluoro substituted complex **23** could be explained with a fast deactivation of the catalytically active centers due to ligand transfer reactions. For **24** bearing two chloro substituents at the iminophenyl rings a dramatically reduced activity was observed compared with the mono-chloro derivative **19**. This result can be explained with a destabilization of the catalytically active species due to the presence of four strong electron withdrawing chloro substituents in the ligand framework. The same tendency was found for the diiodo substituted compound **26** for which the activity reached only half of the activity of the mono-iodo derivative **21**. In contrast to the dichloro derivative **24**, the increased steric bulk provided by four iodo substituents may be responsible for the lower oligomerization activity of the diiodo compound **26**. According to the literature, the highest activities for bis(arylimino)pyridine iron complexes were found for 2-methyl-4-halogen substitution patterns [29,69] and the presence of more than one halogen substituent per iminophenyl ring made explanations of reactivities more difficult, however, it could be stated that combinations of an electron donating group (at *ortho* or *para* position) and an electron withdrawing substituent (at *para* or *ortho* position) within one aryl ring gave the best activities.

For comparison purposes, complexes **22**, **27**, and **28** containing *meta*-alkyl substituted bis(arylimino)pyridine ligands were tested for the oligomerization of ethylene. Since halogen substituents at the *meta*-positions of the iminophenyl rings lead to narrow product molecular weight distributions and, therefore, low values for the Schulz–Flory coefficient α, complexes **22**, **27**, and **28** also revealed to be interesting candidates for ethylene oligomerization reactions. Indeed, these three complexes produced mixtures with very narrow molecular weight distributions ($\alpha = 0.23$ for **22**/MAO and **27**/MAO and $\alpha = 0.20$ for **28**/MAO) indicating high selectivities towards low molecular weight olefins.

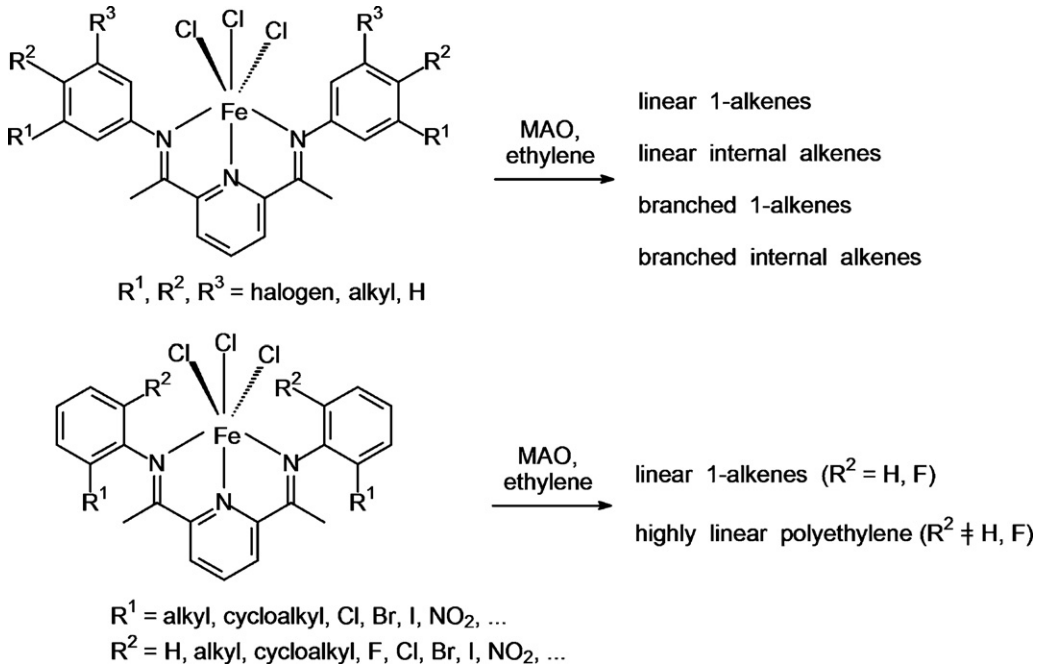

Scheme 8. Dependence of the product compositions on the substitution pattern of the iron(III) catalyst (*meta*- and *para*-substituents were omitted in the lower picture due to their marginal influence when at least one ortho-substituent is present).

*3.4.2. Investigation of the isomerization and cooligomerization behavior of complexes **17–28***

The size of the halogen or alkyl substituents at the iminophenyl rings also effected the isomerization behavior of the bis(arylimino)pyridine iron(III) catalysts. Complexes **17**–**28** as well as the 2-fluoro and all *para*-halogen substituted derivatives produced not only the expected α-olefins, but additionally gave internal and branched olefins (see Tables 4 and 5) due to isomerization and cooligomerization reactions. The lack of *ortho* substituents at the iminophenyl rings can be considered as an essential requirement for this behavior since all complexes containing *ortho*-substituted 2,6-bis(arylimino)pyridine ligands (except the 2-fluoro derivative) produced highly linear products with selectivities for α-olefins above 95% indicating that the *ortho*-substituents are voluminous enough to suppress isomerization reactions of terminal into internal olefins.

Scheme 8 gives a general overview of the product compositions obtained with differently substituted bis(arylimino)pyridine iron(III) complexes. According to theoretical calculations of Ramos [70], bis(arylimino)pyridine iron catalysts bearing *ortho*-methyl substituents on the iminophenyl rings are unable to copolymerize ethylene with higher α-olefins. Additional substituents in *meta*- or *para*-positions (omitted in the lower part of Scheme 8 for clarity) only have a minor influence on the product compositions of such *ortho*-methyl substituted complexes.

For complexes **17**–**28**, the isomerization of α-olefins and the cooligomerization of ethylene with small α-olefins like 1-butene can be verified via GC analyses, since branched and internal alkenes were detected along with the expected 1-alkenes. While the selectivities of catalysts **17**–**28** towards 1-butene in the C-4 fractions always exceeded 98% (Table 4), a closer look on the C_6 fractions gave interesting results. The degree of isomerization of the hexene fraction for the catalytic system **17**/MAO was determined to 50.7% and, correspondingly, the relative amount of 1-hexene in the C_6 fraction was calculated to be only 49.3%. Among the *meta*-monohalogen substituted complexes **18**–**22**, the 3-fluoro and the 3-iodo derivatives (**18** and **21**) exhibited similar tendencies towards the production of C_6 isomers while the 1-hexene content increased dramatically for the 3-bromo compound **20**. Scheme 9 shows the C_6 fraction of the GC spectrum obtained from the oligomer mixture produced with the 3-fluoro compound **18**/MAO along with an assignment of the detected isomers. The assignment was proven by GC analyses of the pure hydrocarbons.

Besides the expected 1-hexene (retention time t_{ret} = 6.42 min), *cis*- and *trans*-2-hexene (t_{ret} ~ 6.60 min and 6.75 min) were identified by comparison of the GC retention times of the pure compounds and further GC/MS correlation using the NIST mass spectral database while 3-hexene (*cis* or *trans*) was not observed.

Isomerization of the terminal 1-hexene into internal C_6 olefins probably proceeds through the coordination of 1-hexene to the iron center and subsequent insertion in a 2,1-mode into the postulated hydrido iron species [7,31,71] followed by β-hydrogen elimination with the two possible pathways *cis*- and *trans*-2-hexene ("chain-running mechanism", see Ref. [72] and Scheme 10).

Branched products additionally require the incorporation of at least one molecule of ethylene or 1-butene into the growing chain before β-hydrogen elimination takes place. Correspondingly, less steric bulk around the iron centers favors this coordination and incorporation (1,2- or 2,1-insertion) of 1-butene. 3-Methyl-1-pentene (t_{ret} ~ 6.10 min) and 2-ethyl-1-butene (t_{ret} ~ 6.60 min) result from cooligomerization reactions of one molecule of ethylene and 1-butene. Starting with a 2,1-insertion of 1-butene followed by incorporation of ethylene and termination through β-hydrogen elimination, 3-methyl-1-pentene is obtained (Scheme 11) which can further be isomerized to give 3-methyl-2-pentene (not detected).

Alternatively, 3-methyl-1-pentene would be accessible from ethylene and 2-butene (*cis* or *trans*). However, the contents of these butene isomers in the mixtures are negligible. 2-Ethyl-1-butene is produced when 1-butene is inserted into an Fe-ethyl bond in a 1,2-mode with subsequent β-hydrogen elimination (Scheme 12).

The presence of the residual C_6 olefins (*cis*- and *trans*-4-methyl-2-pentene, 2-methyl-1-pentene, 2-methyl-2-pentene, 2,3-dimethyl-2-butene) cannot be explained by simple isomerization or cooligomerization reactions of ethylene and butenes. One

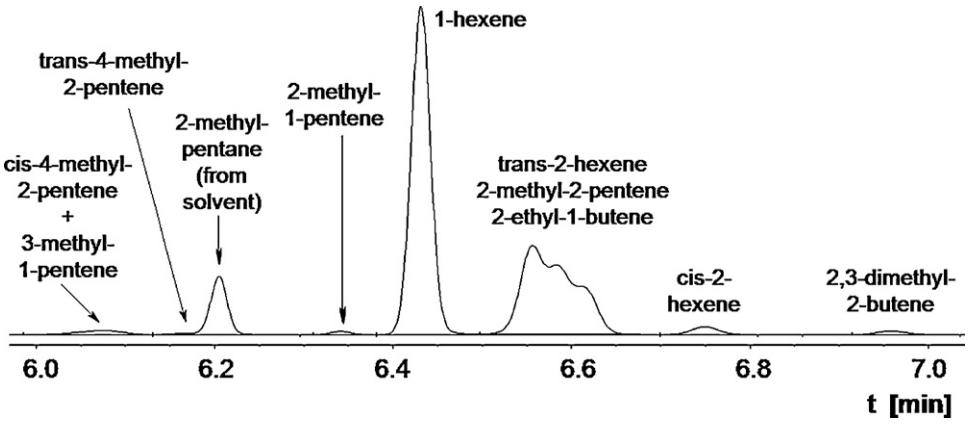

Scheme 9. C_6 region of the GC spectrum of the oligomer mixture produced with **18**/MAO.

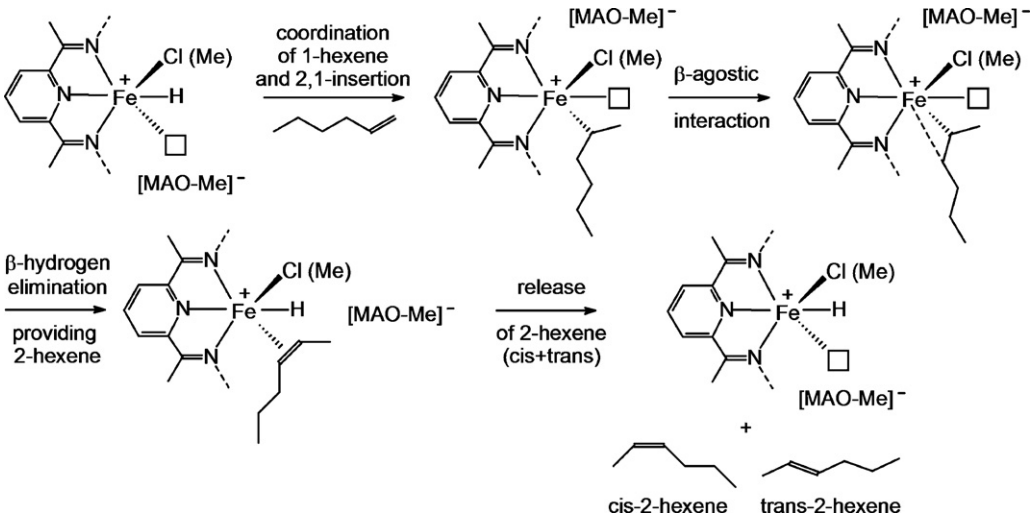

Scheme 10. "Chain-running" of 1-hexene providing internal C_6 isomers [72].

possible reaction pathway to these olefins could be the cleavage of C–C bonds of internal C_6 olefins within the coordination sphere of the iron center yielding C_3 "building blocks" which recombine fast. These assumptions are based on mechanisms presented by Dötterl and Alt [73], Jacobson [74–76], Peake et al. [77], and Grubbs and Miyashita [78] for rearrangement reactions of metallacyclic or metal-bis(olefin) complexes. Dötterl proposed the initial coordination of two ethylene molecules to a formally dikationic nickel center forming a metallacyclopentane. Partial β-hydrogen elimination of that metallacyclic compound provided an alkenyl-hydride species

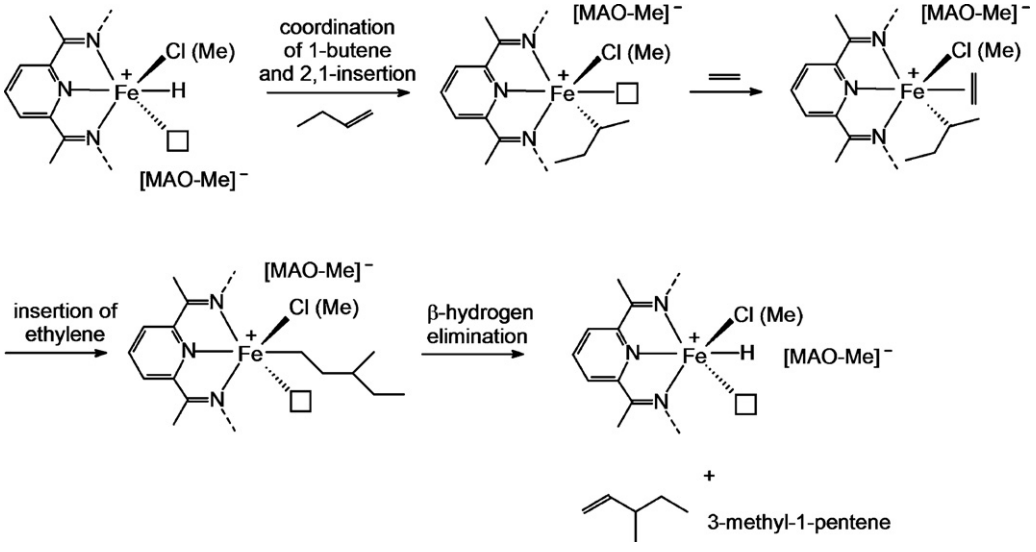

Scheme 11. Cooligomerization of 1-butene and ethylene yielding 3-methyl-1-pentene.

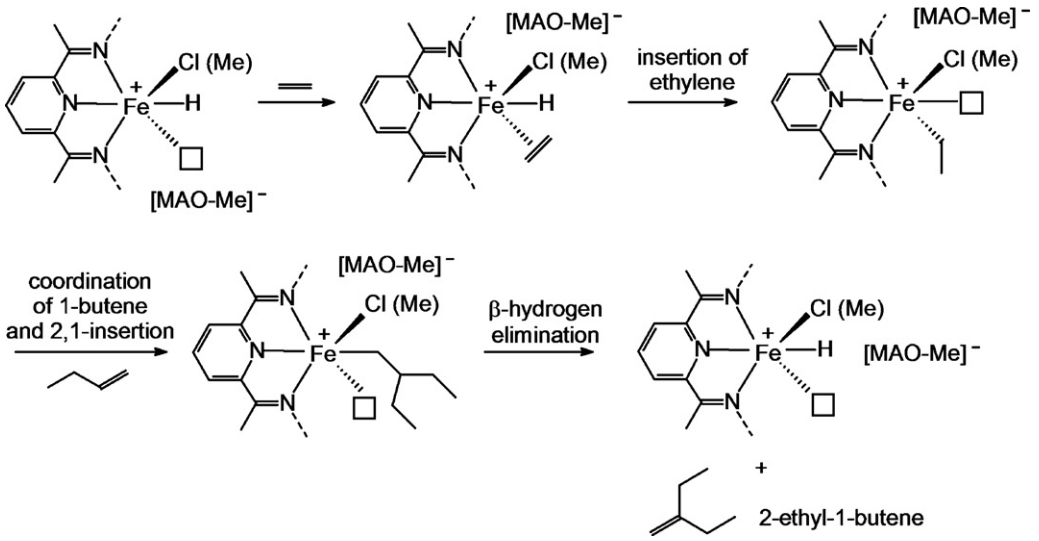

Scheme 12. Cooligomerization of ethylene and 1-butene yielding 2-ethyl-1-butene.

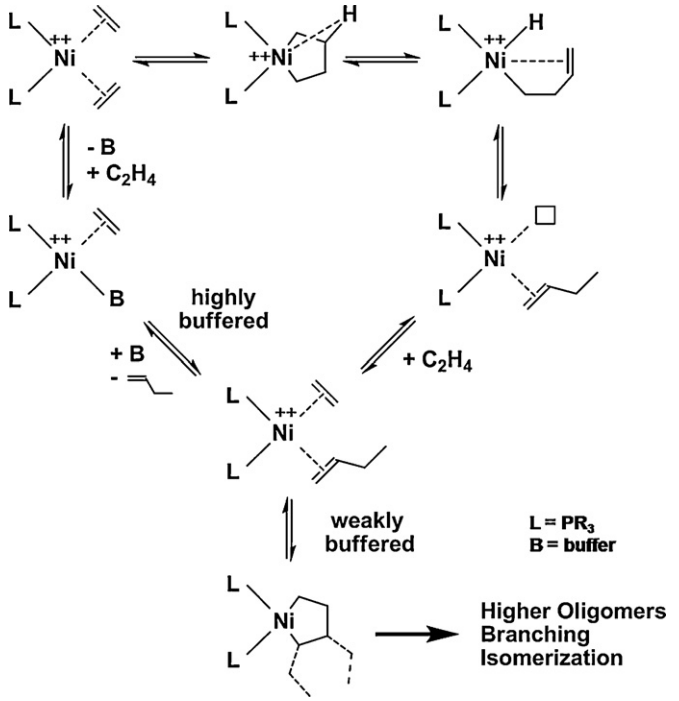

Scheme 13. Mechanism proposed by Dötterl for the MAO-free oligomerization of ethylene in buffered ionic liquids with a formally dikationic nickel complex [73].

which either released 1-butene or coordinated another ethylene molecule forming higher oligomers (see Scheme 13).

In analogy to these "naked" dikationic nickel species, dikationic iron species can also be proposed for bis(arylimino)pyridine iron(III) catalysts. While the pseudo-octahedral coordination sphere of the neutral iron(III) complexes (tridentate bis(arylimino)pyridine ligand and three chloro ligands) has been established (e.g., by Ionkin using crystallography [14,30]), the nature of the third monodentate ligand at the iron atoms after activation with MAO is still unknown. As described in Scheme 7, methylation of the iron(III) catalysts followed by the abstraction of a methyl anion generates a monokationic species with a [MAO-Me]$^-$ cage as the counter anion. At least two of the chloro ligands must have therefore been replaced by methyl groups to start the oligomerization reaction. Very probably, the third chloro ligand is also exchanged against a methyl group due to the excess of MAO.

If that methyl group is then also abstracted by MAO, a dikationic iron(III) species stabilized by two [MAO-Me]$^-$ cages would result which can coordinate two olefin ligands at once. Since two MAO cages are supposed to act as counter anions, there must be enough space for a second cage. In fact, catalysts **17** and **18** featuring the lowest steric bulk around the iron centers apparently fulfil that requirement. The dikationic species may be formed upon the initial activation with MAO (showing a Fe–Me unit) or after one or more catalytic cycles of the commonly accepted monokationic hydrido iron species (Fe-H moiety, see Scheme 14).

The formally dikationic catalyst species is much more destabilized compared with the monokationic species leading to a faster deactivation and, therefore, a lower activity. Both this destabilization and the tendency towards ligand transfer reactions are supposed to be responsible for the comparatively low catalytic activities of complexes **17** and **18**. Despite of its assumed dikationic nature, the catalyst still produces 1-alkenes initially. According to Scheme 13, a metallacycle could be formed easily from a dikationic nickel center and two ethylene molecules. This metallacycle either releases 1-butene or coordinates another ethylene molecule forming 1-hexene or C_6 isomers (depending on the insertion mode of the 1-butene molecule). However, just the presence of an additional ethylene (or 1-butene) molecule in the coordination sphere does not lead to the observed branched isomers. As indicated above, *cis*- and *trans*-2-hexene were detected in the product mixtures. The coordination of either *cis*- or *trans*-2-hexene to the dikationic iron catalyst initially provides an iron-hex-2-yl species. Due to the increased positive charge of the iron center (=strong Lewis acid), stabilization may occur due to activation of an alkyl C–H bond leading to a metallacyclic "ferracyclopentane" intermediate (Scheme 15).

The "dimethylferracyclopentane" species now can convert into a hydrido-bis(propene)iron complex. Depending on the insertion mode of the "propylene intermediates", 2,3-dimethyl-1-butene (twice 2,1-insertion) or 4-methyl-2-pentene and 2-methyl-1-pentene (2,1- and 1,2-insertion) are obtained. 2,3-Dimethyl-1-butene and 2-methyl-1-pentene can be further isomerized to 2,3-dimethyl-2-butene and 2-methyl-2-pentene, respectively (Scheme 16).

One aspect confirming the hypothesis that two alkyl/alkenyl species are involved in the formation of these C_6 olefins could be the presence of 2,3-dimethyl-2-butene in the mixtures

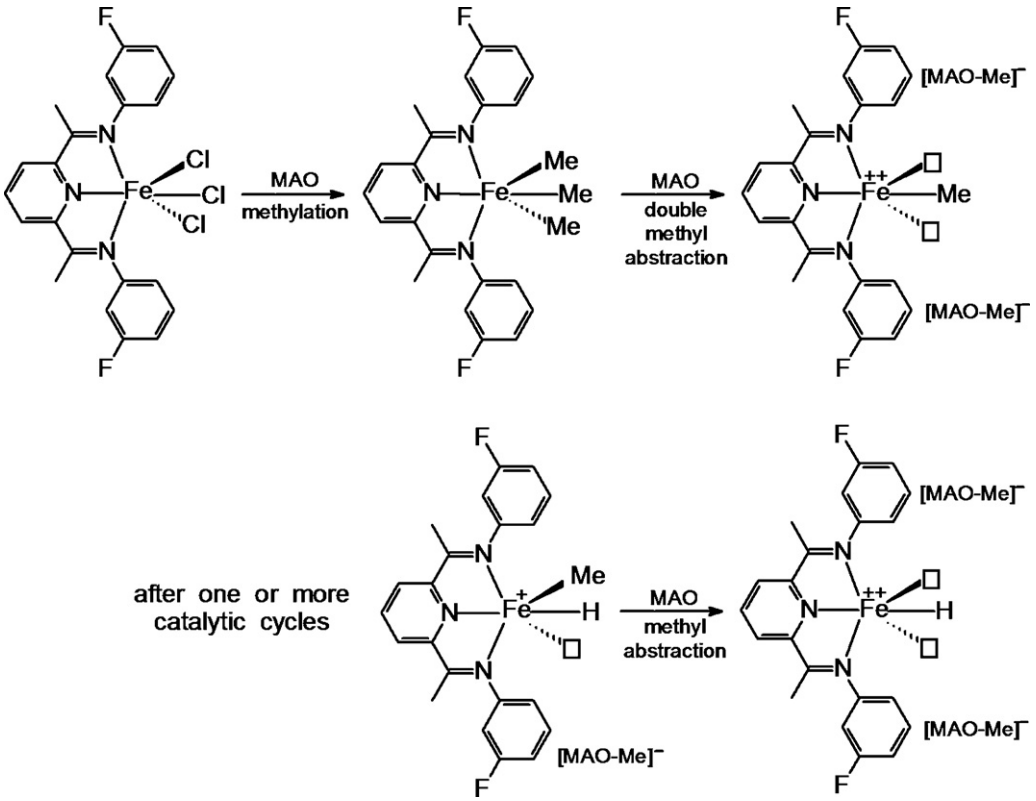

Scheme 14. Proposed formation of a dikationic species from the bis(arylimino)pyridine iron(III) catalyst **18**: initially bearing a Fe–Me group due to the MAO activation (upper picture), after one or more catalytic circles bearing a Fe-H moiety due to β-hydrogen elimination of an olefin (lower picture).

produced with the unsubstituted catalyst **17**, the 3-fluoro derivative **18**, and the *para*-halogen substituted catalysts (see Table 5). Among complexes **17–28**, only catalysts **17** and **18** provide enough space for the formation of the bulky 2,3-dimethylbutene while the steric bulk of all other catalysts prevents its formation. Furthermore, similar product distributions containing *cis*- and *trans*-4-methyl-2-pentene, 2-methyl-1-pentene, 2-methyl-2-pentene, and 2,3-dimethylbutene are obtained with other iron or nickel catalysts in propylene dimerization reactions [73,79–81] while 2-ethyl-1-butene usually cannot be detected in propylene dimerization experiments.

As suggested by a referee, C_3 building blocks may alternatively be formed by an insertion of ethylene into Fe–Me bonds (formed by initial methylation of the trichloride complex with MAO or by regeneration of the catalyst during the oligomerization) and subsequent β-hydrogen elimination of propylene molecules which can then be dimerized. This reaction pathway would also lead to oligomers with odd numbers of carbon atoms since cooligomerization of ethylene and propylene or 1-butene and propylene cannot be excluded. However, according to the GC spectra, C_5 or C_7 alkenes were not found in the product mixtures. In Table 4, there are some examples which show that internal and branched isomers are present in the product mixtures with contents up to 50% of the C_6 fractions (for catalysts **17** and **18**). These contents correspond to molar amounts of more than 100 mmol. Even if all methyl groups of the applied MAO (max. ~ 10 mmol Al) would be used to methylate the iron centers (which is definitely not the case), the isolated amounts of isomers are much higher.

The selectivities of the *meta*-disubstituted complexes **23**–**28** towards α-olefins, especially to 1-hexene, were decisively higher compared with the *meta*-monosubstituted catalysts **18**–**22**. Due to the presence of two *meta* substituents in complexes **23**–**28**, the coordination of higher α-olefins to the iron centers is hindered resulting in lower amounts of isomerized and branched octenes. The exclusive production of 1-octene for **27**/MAO could

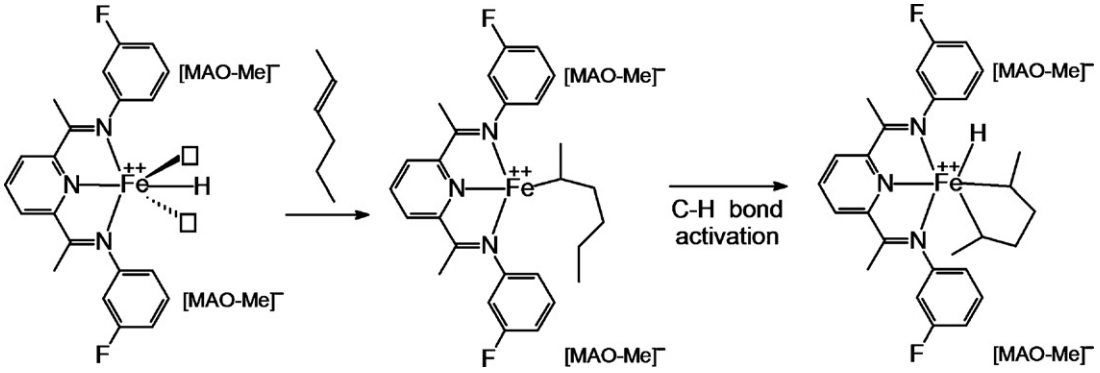

Scheme 15. Proposed formation of a "ferracyclopentane" intermediate.

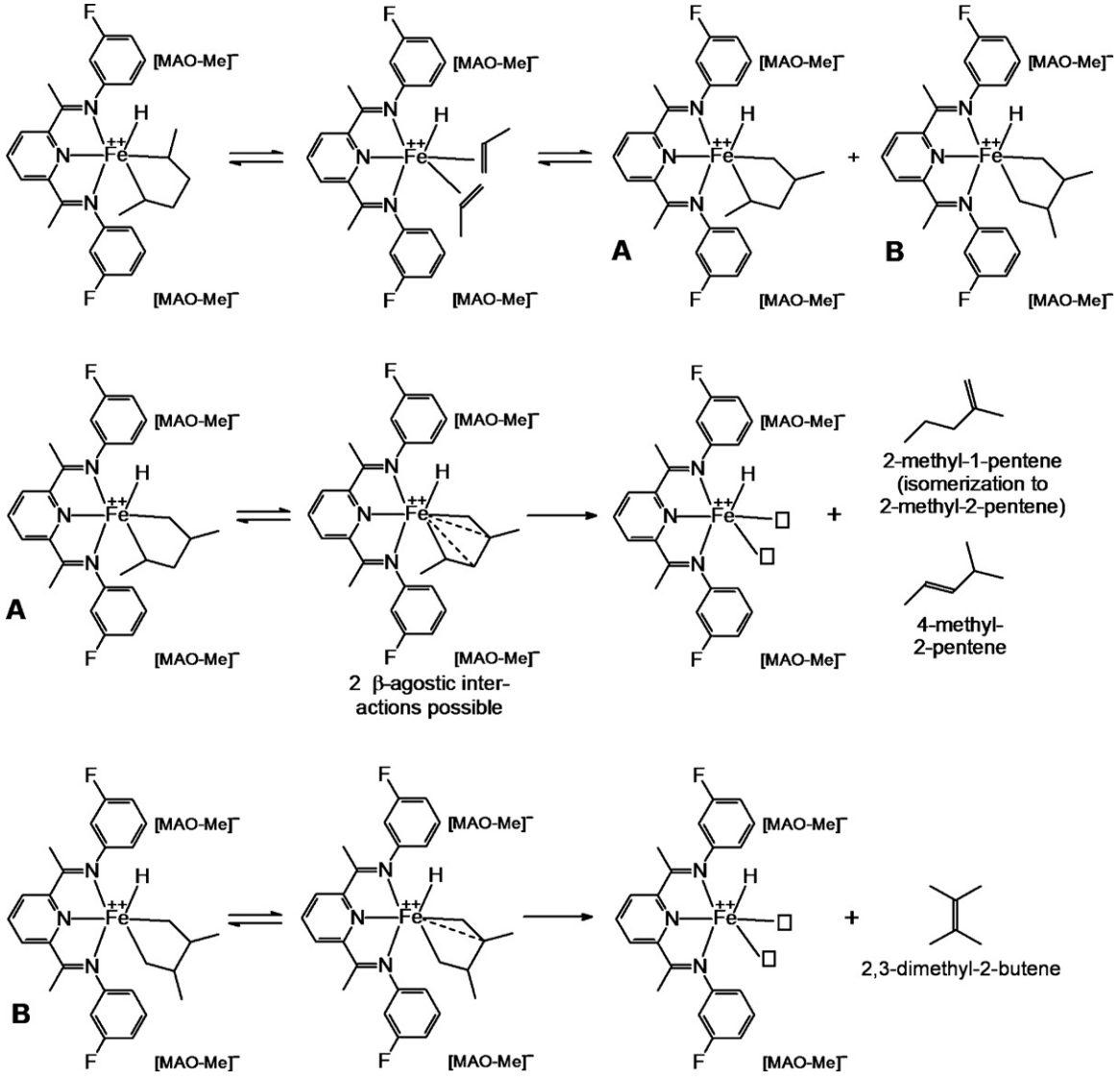

Scheme 16. Proposed formation of methylpentenes and dimethylbutenes over metallacyclic intermediates.

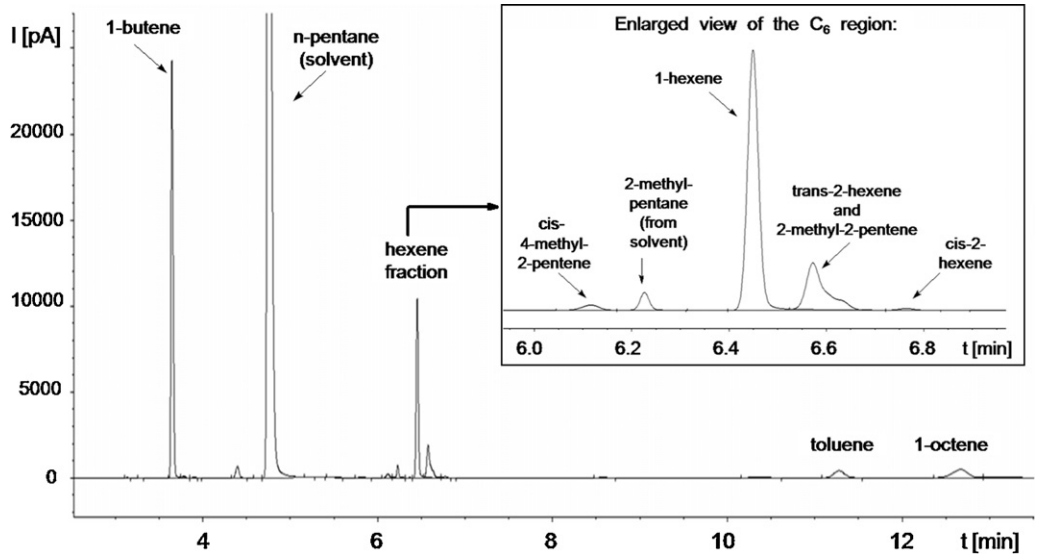

Scheme 17. GC spectrum of the oligomer mixture produced with **25**/MAO (C_4 to C_{10} region; small signals for higher oligomers were omitted for clarity). Offset: enlarged view of the C_6 region (hexenes).

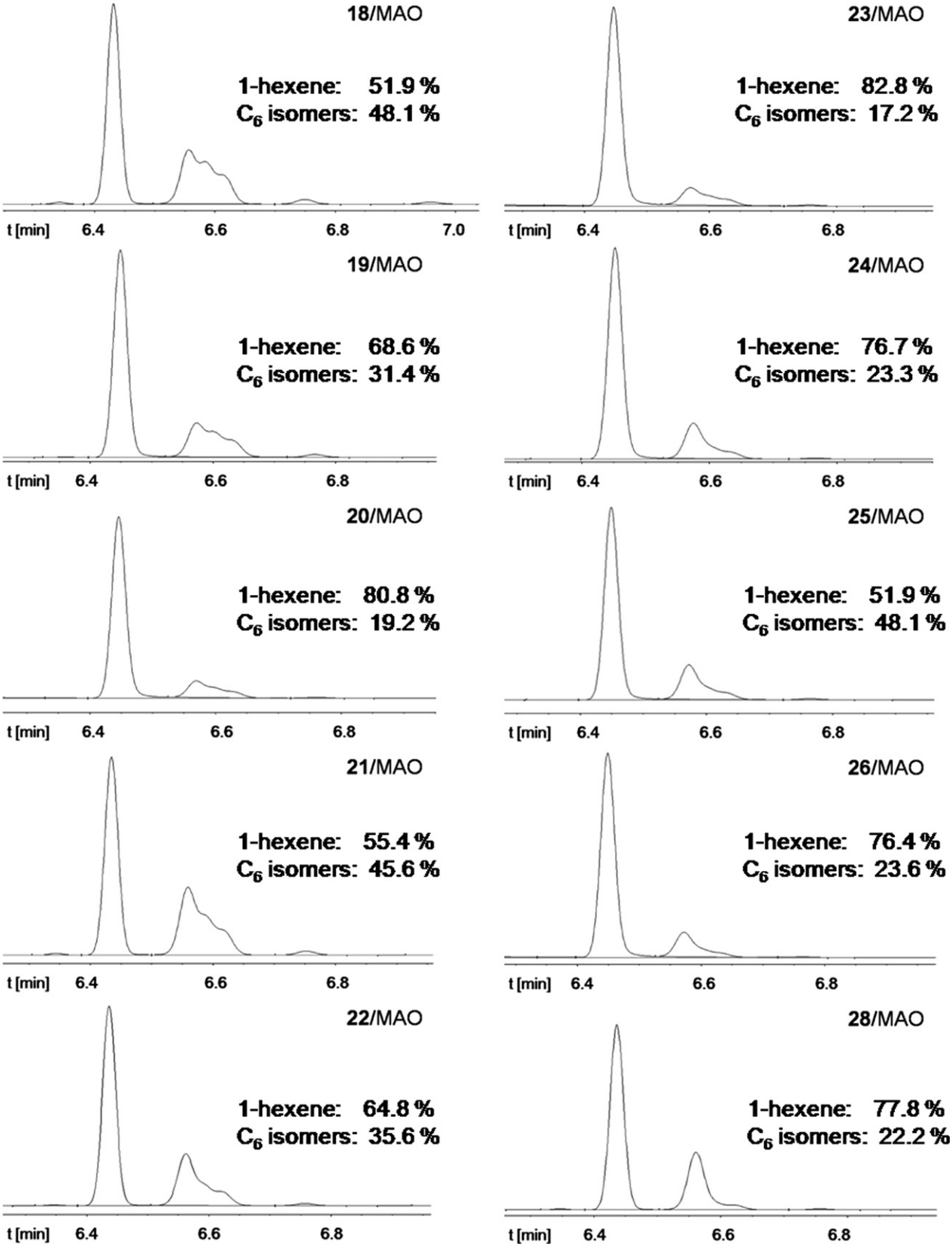

Scheme 18. C_6 regions of the GC spectra of the oligomer mixtures produced with *meta*-monosubstituted (left column) and *meta*-disubstituted catalysts (right column). For the mixture obtained with the 3-fluoro derivative **18**/MAO, the peak for 2,3-dimethyl-2-butene appears at t_{ret} = 6.95 min.

be explained with the quite low activity of the catalyst which is caused by fast deactivation due to ligand transfer reactions. The presence of two bulky tert-butyl groups per iminophenyl ring in complex **28** protects the iron centers moderately from deactivation by ligand transfer reactions leading to a good activity of 20400 [kg prod./mol Fe h].

Scheme 17 shows the GC spectrum of the oligomer mixture produced with **25**/MAO with special attention to the C_6 region. For **25**/MAO, the internal isomers *cis*-2-hexene (t_{ret} = 6.75 min) and *trans*-2-hexene (t_{ret} ~ 6.60 min) as well as the branched isomers 4-methyl-2-pentene (t_{ret} = 6.12 min) and 2-methyl-2-pentene (t_{ret} ~ 6.60 min) were observed. Due to the increased steric bulk of the bromo substituents compared to fluoro or chloro atoms, the content of the "cooligomerization" product 2-ethyl-1-butene significantly decreased (peak around t_{ret} ~ 6.58 missing, see Scheme 9 for comparison) indicating that the 1,2-insertion of 1-butene into the growing chain is hindered (for the subsequent formation of 2-ethyl-1-butene the growing chain is equivalent to an ethyl group). *trans*-4-Methyl-1-pentene, 2-methyl-1-pentene, and 2,3-dimethylbutene were also not found in the mixture produced with **25**/MAO.

Among the iron(III) catalysts shown in Table 5, the *para*-halogen substituted complexes and complex **17** with unsubstituted iminophenyl rings exhibited the greatest tendencies towards isomerization reactions, and remarkably low contents of 1-hexene were found in the C_6 fractions of the product mixtures (always lower than 50%, see Table 5). Compared with the *para*-halogen substituted catalysts, the complexes **18**–**21** afforded increased amounts of 1-hexene (52–81%) in the C_6 fractions (see Table 5). For *meta*-dihalogen substituted catalysts, a further increase of the 1-hexene content could be noted (except for the bromo substituted compounds where the selectivity of the mono-bromo derivative **20** was marginally higher compared with the value for the dibromo derivative **25**). In analogy to the first publications of Brookhart and Gibson [1–7], the *ortho*-substituted compounds showed the highest selectivities towards α-olefins (except the 2-fluoro derivative). For comparison, Scheme 18 shows the enlarged C_6 fractions in the GC spectra obtained for the *meta*-monosubstituted catalysts (**18**–**22**; left) and corresponding *meta*-disubstituted catalysts (**23**–**26** and **28**; right) indicating the increased selectivities towards 1-hexene of the latter ones.

In conclusion, iron(III) complexes with *meta*-substituted iminophenyl rings proved to be highly active catalysts for ethylene oligomerization reactions leading to product mixtures with narrow molecular weight distributions and displayed the ability to isomerize and copolymerize small olefins like 1-butene.

4. Conclusion

Iron(III) complexes containing *meta*-substituted 2,6-bis(arylimino)pyridine ligand frameworks were synthesized and characterized. After activation with methylaluminoxane (MAO), the resulting catalysts proved to be highly active in ethylene oligomerization reactions. Both the size and the electronegativity of the substituents strongly influence the product compositions. Although the iminophenyl rings of the ligand frameworks do not contain substituents in *ortho*-positions to the former amino groups, good catalytic activities were observed. Besides α-olefins, also internal and branched olefins were detected by GC analyses. Explanations for this unusual behavior consider the coordination and insertion of small α-olefins like 1-butene into the growing chains and intermediate C–C bond cleavage reactions. Some of the resulting methylpentenes require the presence of C_3 units in the reaction mixtures which are supposed to form upon coordination of internal C_6 olefins over metallacyclic intermediates. Among this complex type, the *meta*-functionalized 2,6-bis(arylimino)pyridine iron(III) complexes are rare examples which are able to copolymerize ethylene with higher α-olefins and to isomerize terminal into internal olefins.

Acknowledgements

We thank Saudi Basic Industries Corporation (SABIC), Saudi Arabia, for the financial support and Christopher Synatschke (MC II, University of Bayreuth) for recording the MALDI-TOF MS spectra.

References

[1] G.J.P. Britovsek, V.C. Gibson, B.S. Kimberley, P.J. Maddox, S.J. McTavish, G.A. Solan, A.J.P. White, D.J. Williams, Chem. Commun. (1998) 849.
[2] G.J.P. Britovsek, V.C. Gibson, B.S. Kimberley, P.J. Maddox, S.J. McTavish, G.A. Solan, A.J.P. White, D.J. Williams, J. Am. Chem. Soc. 121 (1999) 8728.
[3] G.J.P. Britovsek, V.C. Gibson, D.F. Wass, Angew. Chem. Int. Ed. 37 (1999) 428.
[4] G.J.P. Britovsek, G.K.B. Clentsmith, V.C. Gibson, D.M.L. Goodgame, S.J. McTavish, Q.A. Pankhurst, Catal. Commun. 3 (2002) 207.
[5] B.L. Small, M. Brookhart, J. Am. Chem. Soc. 120 (1998) 7143.
[6] B.L. Small, M. Brookhart, A.M.A. Bennett, J. Am. Chem. Soc. 120 (1998) 4049.
[7] B.L. Small, M. Brookhart, Macromolecules 12 (1999) 2120.
[8] Y. Chen, C. Qian, J. Sun, Organometallics 22 (2003) 1231.
[9] Y. Chen, R. Chen, C. Qian, X. Dong, J. Sun, Organometallics 22 (2003) 4312.
[10] Z. Zhang, S. Chen, X. Zhang, H. Li, Y. Ke, Y. Lu, Y. Hu, J. Mol. Catal. A: Chem. 230 (2005) 1.
[11] F. Pelascini, F. Peruch, P.J. Lutz, M. Wesolek, J. Kress, Eur. Polym. Sci. 41 (2005) 1288.
[12] K. Lappalainen, K. Yliheikkilä, A.S. Abu-Surrah, M. Polamo, M. Leskelä, T. Repo, Z. Anorg, Allg. Chem. 631 (2005) 763.
[13] A.S. Ionkin, W.J. Marshall, D.J. Adelman, A.L. Shoe, R.E. Spence, T. Xie, J. Polym. Sci. A: Polym. Chem. 44 (2006) 2615.
[14] A.S. Ionkin, W.J. Marshall, D.J. Adelman, B. Bobik Fones, B.M. Fish, M.F. Schiffhauer, Organometallics 25 (2006) 2978.
[15] V.C. Gibson, N.J. Long, P.J. Oxford, A.J.P. White, D.J. Williams, Organometallics 25 (2006) 1932.
[16] Y.V. Kissin, C. Qian, G. Xie, Y. Chen, J. Polym. Sci. A: Chem. 44 (2006) 6159.
[17] F.A.R. Kaul, G.T. Puchta, G.D. Frey, E. Herdtweck, W.A. Herrmann, Organometallics 26 (2007) 988.
[18] D. Takeuchi, R. Matsuura, Y. Fukuda, K. Osakada, Dalton Trans. 41 (2009) 8955.
[19] A.S. Ionkin, W.J. Marshall, D.J. Adelman, B. Bobik Fones, B.M. Fish, M.F. Schiffhauer, R.E. Spence, T. Xie, Organometallics 27 (2008) 1147.
[20] D. Takeuchi, R. Matsuura, S. Park, K. Osakada, J. Am. Chem. Soc. 129 (2007) 7002.
[21] K.P. Tellmann, V.C. Gibson, A.J.P. White, D.J. Williams, Organometallics 24 (2005) 280.
[22] M. Seitz, H.G. Alt, A. Aburaqabah, S.J. Palackal, EP 1716924 (2006).
[23] R. Schmidt, B.M. Welch, R.D. Knudsen, S. Gottfried, H.G. Alt, J. Mol. Catal. A: Chem. 222 (2004) 17–25.
[24] M. Lopez Reyes, C. Martin Marcos, O. Prieto Acedo, J. Sancho Royo, J. Campora Perez, P. Palma Ramirez, A.M. Naz Lucena, C.M. Perez Rodriguez, EP 2003166 (2008).
[25] A. Rodriguez-Delgado, J. Campora, A.M. Naz, P. Palma, M.L. Reyes, Chem. Commun. (2008) 5230.
[26] R. Schmidt, U. Hammon, M.B. Welch, H.G. Alt, B.E. Hauger, R.D. Knudsen, US 6458905 (2002).
[27] I.S. Paulino, U. Schuchardt, J. Mol. Catal. A: Chem. 211 (2004) 55.
[28] Z. Zhang, J. Zou, N. Cui, Y. Ke, Y. Hu, J. Mol. Catal. A: Chem. 219 (2004) 249.
[29] C. Goerl, H.G. Alt, J. Organomet. Chem. 692 (2007) 4580.
[30] A.S. Ionkin, W.J. Marshall, D.J. Adelman, B. Bobik Fones, B.M. Fish, M.F. Schiffhauer, P.D. Soper, R.L. Waterland, R.E. Spence, T. Xie, J. Polym. Sci. A: Polym. Chem. 46 (2008) 585.
[31] C. Goerl, H.G. Alt, J. Mol. Catal. A: Chem. 273 (2007) 118.
[32] A.S. Ionkin, WO 2007059015 (2007).
[33] D.D. Devore, S.S. Feng, K.A. Frazier, J.T. Patton, WO 2000069923 (2000).
[34] K.P. Bryliakov, N.V. Semikolenova, V.N. Zudin, V.A. Zakharov, E.P. Talsi, Catal. Commun. 5 (2004) 45.
[35] F. Prades, R. Spitz, C. Boisson, S. Sirol, A. Razavi, WO 2007014889 (2007).
[36] D. Gong, B. Wang, C. Bai, J. Bi, F. Wang, W. Dong, X. Zhang, L. Jiang, Polymer 50 (2009) 6259.
[37] P. Hao, Y. Chen, T. Xiao, W.-H. Sun, J. Organomet. Chem. 695 (2010) 90.
[38] C. Goerl, T. Englmann, H.G. Alt, J. Appl. Catal. A: Gen. 403 (2011) 25.
[39] E.P. Talsi, D.E. Babushkin, N.V. Semikolenova, V.N. Zudin, V.N. Panchenko, V.A. Zakharov, Macromol. Chem. Phys. 202 (2001) 2046.
[40] J. Martinez, V. Cruz, J. Ramos, S. Gutierrez-Oliva, J. Martinez-Salazar, A. Toro-Labbe, J. Phys. Chem. C 112 (2008) 5023.
[41] V. Cruz, J. Ramos, J. Martinez-Salazar, S. Gutierrez-Oliva, A. Toro-Labbe, Organometallics 28 (2009) 5889.
[42] R. Raucoules, T. de Bruin, P. Raybaud, C. Adamo, Organometallics 27 (2008) 3368.
[43] I.E. Soshnikov, N.V. Semikolenova, A.N. Bushmelev, K.P. Bryliakov, O.Y. Lyakin, C. Redshaw, V.A. Zakharov, E. Talsi, Organometallics 28 (2009) 6003.

[44] M. Seitz, C. Goerl, W. Milius, H.G. Alt, Jordan J. Chem. 3 (2008) 109.
[45] A.S. Abu-Surrah, K. Lappalainen, U. Piironen, P. Lehmus, T. Repo, M. Leskelä, J. Organomet. Chem. 648 (2002) 55.
[46] R.-F. Chen, C.-T. Qian, J. Sun, Chin. J. Chem. 19 (2001) 866.
[47] M.E. Bluhm, C. Folli, M. Döring, J. Mol. Catal. A: Chem. 212 (2004) 13.
[48] B. Cetinkaya, E. Cetinkaya, M. Brookhart, P.S. White, J. Mol. Catal. A: Chem. 142 (1999) 101.
[49] O. Dayan, F. Dogan, I. Kaya, B. Cetinkaya, Syn. React. Inorg. Metal-Org. Nano-Metal Org. Chem. 40 (2010) 337.
[50] A.S. Ionkin, L.K. Johnson, US 2006/0009597 (2006).
[51] J. Jia, CN 2003-105297 20030228 (2004).
[52] C. Liu, G. Zhou, G.X. Jin, CN 1306012 (2001).
[53] D.R. Haydon, L.G. Czaplewski, N.J. Palmer, D.R. Mitchell, J.F. Atherall, C.R. Steele, T. Ladduwahetty, WO 2007148093 (2007).
[54] R. Schmidt, M.B. Welch, S.J. Palackal, H.G. Alt, J. Mol. Catal. A: Chem. 179 (2002) 155.
[55] C. Qian, F. Gao, Y. Chen, L. Gao, Synlett (2003) 1419.
[56] G.-X. Jin, C. Liu, CN 1352204 (2002).
[57] R.F. Moreira, E.Y. Tshuva, S.J. Lippard, Inorg. Chem. 43 (2004) 4427.
[58] R. Li, R.L. Smith, H.I. Kenttamaa, J. Am. Chem. Soc. 116 (1996) 5056.
[59] V. Malatesta, K.U. Ingold, J. Am. Chem. Soc. 103 (1981) 609.
[60] G.V. Schulz, Z. Phys. Chem. B 30 (1935) 379.
[61] G.V. Schulz, Z. Phys. Chem. B 43 (1939) 25.
[62] P.J. Flory, J. Am. Chem. Soc. 62 (1940) 1561.
[63] H. Kehlen, M.T. Rätsch, Z. Phys. Chem. 256 (1984) 1049.
[64] M. Seitz, Diploma thesis, University of Bayreuth, Germany, 2001.
[65] S.A. Svejda, M. Brookhart, Organometallics 18 (1999) 65.
[66] G. Henrici-Olive, S. Olive, Adv. Polym. Sci. 15 (1974) 1.
[67] S. Peitz, N. Peulecke, B.R. Aluri, S. Hansen, B.H. Mueller, A. Spannenberg, U. Rosenthal, M.H. Al-Hazmi, F.M. Mosa, A. Woehl, W. Mueller, Eur. J. Inorg. Chem. (2010) 1167.
[68] T. Zhang, W.H. Sun, T. Li, X.J. Yang, J. Mol. Catal. A: Chem. 218 (2004) 119.
[69] M. Watanabe, H. Sato, M. Kuramoto, H. Tashiro, S. Tanaka, T. Tamura, WO 2001017967 (2001).
[70] J. Ramos, V. Cruz, A. Munoz-Escalona, J. Martinez-Salazar, Polymer 43 (2002) 3635.
[71] B.L. Small, A.J. Marcucci, Organometallics 20 (2001) 5738.
[72] C.M. Killian, L.K. Johnson, M. Brookhart, Organometallics 16 (1997) 2005.
[73] M. Dötterl, H.G. Alt, ChemCatChem (2011), doi:10.1002/cctc.201100182.
[74] D.B. Jacobson, B.S. Freiser, Organometallics 3 (1984) 513.
[75] D.B. Jacobson, B.S. Freiser, J. Am. Chem. Soc. 105 (1983) 736.
[76] D.B. Jacobson, B.S. Freiser, J. Am. Chem. Soc. 105 (1983) 5197.
[77] D.A. Peake, M.L. Gross, D.P. Ridge, J. Am. Chem. Soc. 106 (1984) 4307.
[78] R.H. Grubbs, A. Miyashita, J. Am. Chem. Soc. 100 (1978) 7416.
[79] H.G. Alt, K.J. Schneider, E. Funk, Jordan J. Chem. 3 (2008) 367.
[80] H.G. Alt, K.J. Schneider, C. Goerl, Jordan J. Chem. 4 (2009) 33.
[81] M. Dötterl, H.G. Alt, Adv. Synth. Catal., doi:10.1002/adsc.201100557.